

hochschule mannheim



The impact of various meteorological years on system reliability in a German energy scenario for 2025

David Treuherz

Bachelor Thesis

for the acquisition of the academic degree Bachelor of Science (B.Sc.)

Course of Studies: Power Engineering and Renewable Energies

Department of Electrical Engineering
University of Applied Sciences Mannheim

11.09.2015

Tutors

Prof. Dr. Hermann Merz, Hochschule Mannheim

Karl-Kiên Cao and Felix Cebulla, Deutsches Zentrum für Luft- und Raumfahrt

Treuherz, David:

Der Einfluss unterschiedlicher Wetterjahre auf die Versorgungssicherheit eines deutschen
Energieszenarios für 2025 / David Treuherz. –

Bachelor Thesis, Stuttgart : University of Applied Sciences Mannheim, 2013. 55 pages.

Treuherz, David:

The impact of various meteorological years on system reliability in a German energy sce-
nario for 2025 / David Treuherz. –

Bachelor Thesis, Stuttgart : Hochschule Mannheim, 2013. 55 Seiten.

Erklärung

Hiermit erkläre ich, dass ich die vorliegende Arbeit selbstständig verfasst und keine anderen als die angegebenen Quellen und Hilfsmittel benutzt habe.

Stuttgart, 11.09.2015

David Treuherz

Abstract

Der Einfluss unterschiedlicher Wetterjahre auf die Versorgungssicherheit eines deutschen Energieszenarios für 2025

Versorgungssicherheit eines Energiesystems ist gegeben, wenn die Nachfrage an Energie jederzeit gedeckt werden kann. In dieser Arbeit wird ein deutsches Energieszenario für 2025 mit hohen Anteilen fluktuierender erneuerbarer Energiequellen, vor allem Wind und Photovoltaik, hinsichtlich des Einflusses unterschiedlicher Wetterjahre auf die Versorgungssicherheit untersucht. Als Messzahl der Versorgungssicherheit dient die „loss of load expectation“ (LOLE). Für die Berechnung des LOLEs wird eine analytische Methode für ein deutsches Energieszenario angewendet, um den Einfluss von unterschiedlichen Wetterjahren zu bestimmen. Die Ergebnisse zeigen, dass die Versorgungssicherheit erheblich durch das verwendete Wetterjahr beeinflusst wird.

Zusätzlich können statistische Zusammenhänge zwischen den Wetterjahren und der Versorgungssicherheit festgestellt werden. Des Weiteren wird in dieser Arbeit die Beeinflussung der Versorgungssicherheit durch Abregelung und Lastausgleich untersucht. Inwiefern ein deutsches Energieszenario für 2025 Versorgungssicher ist, wird mit Hilfe des Energiesystemmodells REMix untersucht. Die Ergebnisse zeigen einen starken Einfluss von Lastausgleichsoptionen auf die Versorgungssicherheit. Die LOLE wird nahezu auf Null gesenkt.

The impact of various meteorological years on system reliability in a German energy scenario for 2025

System reliability describes the ability of an energy system to meet its demand at any time. In this thesis, a German energy scenario for 2025 with large shares of fluctuating renewable energy sources, in particular wind and photovoltaic, is analyzed regarding the influence of historical meteorological input data on system reliability. Using the loss of load expectation approach (LOLE) for a German energy scenario an assessment of the influence of various meteorological years on system reliability is carried out. The results indicate a significant impact of the used meteorological year on the LOLE.

Furthermore the interdependency of curtailment and load balancing on system reliability is investigated. Therefore a LOLE for a German energy scenario for 2025 considering curtailment and flexibility options is calculated using the energy system

model REMix. The outcome reveals a large influence of load balancing on system reliability. The loss of load expectation is reduced to almost zero.

Contents

Abbreviations	vii
1. Introduction	1
2. State of research	5
2.1. Capacity value	5
2.2. Loss of load expectation	7
3. Methodology	9
3.1. Loss of load expectation	9
3.1.1. Capacity outage probability table	9
3.1.2. Residual load duration curve	11
3.1.3. Loss of load expectation calculation	12
3.2. Constrained loss of load expectation	14
3.3. Correlation between meteorological years and system reliability . .	14
3.4. Energy system model REMix	16
3.5. Balanced loss of load expectation	17
3.6. Used data	19
3.6.1. Data sources	19
3.6.2. Data input	19
4. Results	25
4.1. Analysis of individual meteorological years	25
4.1.1. Power generation	25
4.1.2. Annual energy	27
4.1.3. Gradients	29
4.2. Analysis of the time period 2006 - 2012	30
4.2.1. Annual energy	30
4.2.2. Gradients	32
4.3. Constrained loss of load expectation for 2025	35
4.4. Balanced loss of load expectation for 2025	37
4.5. Correlation between meteorological years and system reliability . .	40
4.5.1. Constrained loss of load expectation	40
4.5.2. Balanced loss of load expectation	41

4.6. Discussion	42
4.6.1. Influence of meteorological years on system reliability	42
4.6.2. The impact of load balancing on system reliability	44
5. Conclusion	49
6. Outlook	53
6.1. Analysis of meteorological years	53
6.2. REMix scenario	54
6.3. Analysis of system reliability	54
Bibliography	57
Appendices	61
A. Capacity outage probability table	63
B. Loss of load expectation Python script	67
C. REMix input	71
List of figures	75
List of tables	76

Abbreviations

RE renewable energy

REMix Renewable Energy Mix for Sustainable Electricity Supply

DLR Deutsches Zentrum für Luft- und Raumfahrt

LOLE loss of load expectation

CV capacity value

COPT capacity outage probability table

FRE fluctuating renewable energy

FOR forced outage rate

RLDC residual load duration curve

LOLP loss of load probability

GFRE potential electricity generation time series of fluctuating renewable energy sources

EUMENA Europe, Middle East and North Africa

EnDAT Energy Data Analysis Tool

OptiMo Optimization Model

AC alternating current

DC direct current

PS pumped storage

CCGT combined cycle gas turbine power plants

GT-NGas natural gas power plants

ST-Coal coal-fired steam turbine power plants

ST-Lignite lignite-fired steam turbine power plants

CNE Central and North Europe

ENTSO-E European Network of Transmission System Operators for Electricity

RG regional group

Contents

RRH run of river hydro

MW megawatts

STD standard deviation

MWh megawatt-hours

TWh terawatts-hours

GWh gigawatt-hours

GW gigawatts

Chapter 1

Introduction

Since the first power generation for public customer meeting energy demand has been one of the major challenges for the energy economy. Today, in the early twenty-first century, the demand for energy is higher than ever before and there is the tendency that it will still increase [27]. Besides the challenge of meeting energy demand, sustainable energy supply has moved more and more into focus of science and policymakers during the last decades. There are several facts why energy policy has changed and is still changing. On the one hand due to the significant increasing emission rate of CO_2 climate change has become an all global issue. Fossil fuel is the primary source of carbon dioxide and especially the energy sector with its high share of fossil fired power plants which burn gas or different kinds of coal, has a crucial negative impact on climate change. On the other hand one must consider the finite supply of fossil fuel. Still in the year 2013 the European Union received 76.8 % [13] of its energy from conventional power generation.

But especially Germany, one of Europe's leading countries in the expansion of renewable energy (RE) technologies, increases its shares of RE in power generation constantly. "Energiewende" (energy transition) is the name for the long-term change in the German energy system. The government formulated ambitious goals in the recent years: Until 2025 the shares of REs in the power sector should increase up to 40 to 45 % and should reach 55 to 60 % in 2035 [5].

Energy system models are one possible method to create and analyze feasible goals for the German energy transition. These models apply different techniques, including "mathematical programming (usually linear programming), activity analysis, econometrics, and related methods of statistical analysis" [18]. Renewable Energy Mix for Sustainable Electricity Supply (REMIX) is the energy system model which

is used in this bachelor thesis. REMix was developed at the German Aerospace Center (Deutsches Zentrum für Luft- und Raumfahrt (DLR)) and dimensions low-cost power supply structures. Since REMix minimizes the total costs of an energy system, it determines the dispatch of power generation technologies and power balancing options. In addition, it is also applicable for capacity expansion studies.

Since the promotion and development of REs in Europe is steadily increasing, the impact of the weather on the European energy supply is increasing at the same time. Energy system models often use historical meteorological data as input for the determination of power generation of REs in the future. Usually, REMix uses one weather year for all related studies and no detailed assessment (e.g. sensitivity analyses) regarding this input parameter has been done, yet.

One main focus of this thesis is on investigating the impact of meteorological data on a typical outcome of REMix, which is the reliability of an energy system. Therefore the loss of load expectation (LOLE) is selected as an indicator to describe the system stability of a German energy scenario for the year 2025. On the one hand the impact of weather conditions on a constrained German energy system without considering load balancing options is determined. For an energy system with high shares of REs it is likely that weather conditions have a large influence on system reliability. On the other hand the impact of meteorological years on a German energy system including balancing options is analyzed by applying linear optimization model REMix.

Another aspect is in how far the system reliability differs when using REMix to determine the LOLE. Due to load balancing options, such as storage, curtailment and electricity export as well as imports, the system reliability will presumably be affected.

There exist different metrics to assess the influence of weather conditions on energy systems. In addition to the LOLE the capacity value (CV) is introduced in the following literature review. The CV approach describes the contribution of one generation technology in periods of peak demand. In chapter 3, the developed methodologies on basis of the current state of research are explained in detail. The calculation method of the capacity outage probability table (COPT) and the methodology of calculating the constrained LOLE is shown for a restricted German energy system as well as for a energy system which considers balancing options. In addition the input data and their sources for both LOLE approaches are listed. In the first two

parts of Chapter 4, the meteorological years are characterized and depicted. In connection with this characterization, the relations between each LOLE approach and the input weather data are analyzed. Finally, the impact of load balancing is analyzed and the results of all investigations are discussed furthermore an outlook for further investigations is given.

Chapter 2

State of research

In order to assess the impact of weather conditions, or the impact of climate on energy systems, an increasing number of research institutes, universities and scientists have published papers and articles on this topic in the recent years. Michaelis, Plötz and Müller (Frauenhofer Institute for Systems and Innovation Research) examined the influence of historical wind feed-in time series and load on spot market prices for 2030. They used different base years for the simulation runs. The outcome of this examination confirmed that the characteristics of the price time series are highly correlated to the chosen wind feed-in time series [22]. Brouwer et al. quantified the impacts of large-scale intermittent RE sources on electricity systems. It is noted that it is important to analyze multiple weather years for an accurate quantification of capacity value of RE sources [4]. The following sections deal with the capacity value and thus with system reliability and its sensitivity to weather conditions.

2.1. Capacity value

The CV expresses the ability of a power plant to provide capacity to an energy system in periods of peak demand. An energy system is reliable, if the electrical demand can be met by the available capacity at anytime. Conventional power plants such as gas fired or coal-fired power plants are dispatchable and have a substantial contribution to system reliability.

While accelerating the expansion of RE sources and reducing dispatchable conventional power generation at the same time, the maintenance or the improvement of system reliability of energy systems is of great interest to energy companies and

2. State of research

to transmission system operators. With increasing shares of fluctuating renewable energy (FRE) sources, the question arises which contribution to system reliability does wind and photovoltaic power plants have. Due to the high theoretical potential of wind power in parts of the United States several institutions evaluated the operational impact of increasing wind energy penetration on the power system in the next decades. The CV of wind generation at different penetration levels was therefore determined in [10] and [15].

Forced outage rate

The forced outage rate (FOR) of conventional power plants is an essential factor for determining the CV. Due to outages conventional power plants are not 100 % available during 8,760 hours of a year. The FOR, expressed in percentage, captures two kinds of possible outage events. Either the power plant or just one unit of the power plant is taken out of service for maintenance or replacement (called “planned outages”) or the unit is out of service due to failure (called “unplanned outage”) [25]. The formula for calculating the FOR is shown in Equation 2.1. For RE sources such as wind power, “unplanned outages” occur if the wind is not blowing. Thus outages of a wind plant are mostly based on weather conditions and not on power plant failure. Weather is very changeable, methods for its prediction are associated with uncertainties and weather patterns vary from year to year. Hence the CV of intermittent RE sources need to be calculated with another method.

$$FOR = \frac{\text{forced outage hours}}{\text{in service hours} + \text{forced outage hours}} \quad (2.1)$$

Capacity value for renewable energies

Different approaches for determining the capacity value for renewable power plants exist, such as the Effective Capacity Method [24]. The advantage of this method is that the temporal and seasonal fluctuation of wind plant output is captured. The system reliability indicator LOLE is an essential metric for this retrospective approach and is used as system reliability target for calculating the CV of RE sources.

EnerNex Corporation in collaboration with the Midwest Independent System Operator published a wind integration study for Minnesota [10]. One goal of CV analysis is to review inter-annual variations. EnerNex uses three different meteorological years (2003 - 2005) to provide a better characterization of the wind power

generation during periods of peak demand. The variation of the annual CVs for the different years at a wind penetration level of 15 % is about 16 %. It is noted, that this variation is likely caused by meteorological conditions, as it can affect both electric demand and wind generation. The “Western Wind and Solar Integration Study” prepared by GE Energy analyses the CV is based on historical weather data of three years as well (2004 - 2006) [15]. Their resulting CVs in the monthly resolution show significant year-to-year variations, but no further investigations concerning the impact of meteorological years on the CV is done.

The input data which is required for calculating the CV of wind power includes load time series for the period of investigation, wind power times series for the same period, a complete inventory of conventional power plants (generation units' capacity) and their forced outage rates [19]. Considering the temporal resolution, in [17] it is stated that the weather data should have a resolution of 1 hour or less and at least four to five years of data should be used for stable calculations.

If the CV gets calculated with a benchmark unit as in the Effective Capacity Method, one can say that the CV describes the size of a gas power plant which would be capable to replace the wind power plants while maintaining the same system reliability. By definition the CV method only considers one RE source – for evaluating the impact of various meteorological years on energy systems with high shares of RE sources it is essential to investigate the impact of photovoltaic and wind power at the same time. Therefore the CV method is not suitable and it is advantageous to use the LOLE as metric.

2.2. Loss of load expectation

In the last few years, LOLE has become an important metric to monitor system reliability in Germany and its neighbouring countries [23]. System reliability is a key element in recent reports of the German transmission system operators [6]. Their proposed indicator for the monitoring of system reliability is LOLE. The Pentalateral Energy Forum assessed generation adequacy for Germany and six neighbouring countries [23]. Regional adequacy assessment for 2015/2016 and 2020/2021 comprises detailed LOLE analysis. No investigations dealing with the impact of different meteorological years are done. But it is mentioned, that their methodology

2. State of research

is still open to further improvements such as the extension of the climate database to cover more climatic variations.

EnerNex Corporation published a wind integration and transmission study in 2010, examining the operational impact of increasing wind penetration rates up to 30 % in 2024 on the power system in the Eastern Interconnection of the United States [7]. This technical report states that the accepted industry standard for a reliable system is less than one day in ten years, which are 2.4 hours per year. In this thesis this benchmark is used as a standard for a reliable system as well.

LOLE describes the expectation of a loss of load event [19]. These are events in which the load will exceed the available generation and thus a low LOLE indicates a high system reliability. Usually LOLE is considered over a defined time period and is expressed in hours per year or days per year. Common system reliability evaluations are based on a probabilistic approach. There are two kinds of approaches which use probabilistic evaluations. On the one hand Monte Carlo Simulations are a stochastic method, where system reliability indexes are determined by simulating the actual process and random behavior of the energy system. On the other hand analytical methods represent the system by mathematical models. System reliability indexes are calculated from the model by using direct analytical solutions [24]. The applied analytical method for calculating LOLE is described and illustrated in the following section 3.1.

Chapter 3

Methodology

3.1. Loss of load expectation

As mentioned in section 2.2, system adequacy and therefore system reliability is an important factor in long-term planning of future energy systems. The applied method for calculating system reliability indicator LOLE can be divided in two parts. These two parts are not built on each other, but rather combined at the end of the calculation process. One part is simply the residual load duration curve (RLDC), and the other is the COPT. Both models are implemented in Python. Python is a programming language with a large number of libraries and with Python's open source library pandas, tools for data structures and data analysis are provided, which meet the requirements for calculating LOLE for this thesis.

3.1.1. Capacity outage probability table

The COPT is a table which contains the outage capacity states of a whole energy system and their probabilities in an ascending order of outage magnitudes. Therefore, COPT is based on all conventional power plant technologies of the considered energy system. Each technology has its FOR and is divided into power plant units. With an iterative algorithm based upon discrete distribution developed by Wang and McDonald published in [28], the exact probability of every outage state can be calculated.

This algorithm can be demonstrated by the following example:

3. Methodology

Example COPT:

Generating units of the energy system:

Unit A: 10 MW, FOR = 0.02, Availability = 0.98.

Unit B: 20 MW, FOR = 0.01, Availability = 0.99.

Unit C: 25 MW, FOR = 0.03, Availability = 0.97.

COPT of this energy system:

Outage Capacity (MW)	Probability
0	$0.98 \cdot 0.99 \cdot 0.97 = 0.94109$
10	$0.02 \cdot 0.99 \cdot 0.97 = 0.01921$
20	$0.98 \cdot 0.01 \cdot 0.97 = 0.00951$
25	$0.98 \cdot 0.99 \cdot 0.03 = 0.02911$
30	$0.02 \cdot 0.01 \cdot 0.97 = 0.00019$
35	$0.02 \cdot 0.99 \cdot 0.03 = 0.00059$
45	$0.98 \cdot 0.01 \cdot 0.03 = 0.00029$
55	$0.02 \cdot 0.01 \cdot 0.03 = 0.00001$

Table 3.1.: Example capacity outage probability table calculation.

The energy system used in this example consists of 3 units with a total installed capacity of 55 megawatts (MW). Considering a German energy system of 2025, the installed capacity of dispatchable power plants is more than one thousand times higher than in this example energy system. To calculate the COPT of an energy system of this size, equation 3.1 captures the applied iterative algorithm [20]. For this thesis this algorithm is implemented in Python. The Python script can be found in appendix A as well as sections of the computed COPT for the German energy scenario for 2025 (Table A.1).

$$p_n(X) = p_{n-1}(X) \cdot p(0) + p_{n-1}(X - C_n) \cdot p(C_n) \quad (3.1)$$

The recurrence of the algorithm is due to the iterative addition of generating units. With each added unit the exact probability of the system outage capacity $p_n(X)$ is recalculated. A state is considered, where $n - 1$ generating units have already been added to the table. The exact probability that a capacity of X is on outage is $p_{n-1}(X)$. For explanation equation 3.1 can be divided into two parts. The first addend describes the case that the new unit is available and all already added units have an outage capacity of X . So the probability of $p_{n-1}(X)$ is multiplied with the probability $p(0)$ that the new unit is available. In the second case (second addend),

the new unit is on outage. The capacity C_n of the new unit is not available with a probability of $p(C_n)$, which is the FOR of this unit. Since the new unit is on outage, the already added units are just on an outage capacity of $X - C_n$ to have the sum outage capacity of X . This probability is expressed with $p_{n-1}(X - C_n)$. By summing the probabilities of both cases, the exact probability of the outage capacity X is obtained.

Equation 3.1 can be also used for calculating the cumulative probability $P_n(X)$, which describes the probability that the capacity X or more is on outage. Therefore $p_{n-1}(X)$ and $p_{n-1}(X - C_n)$ are changed to the corresponding cumulative state probabilities. In the event that $X \leq C_n$, it is stipulated for the exact probability that $p_{n-1}(X - C_n) = 0$ and that $p_{n-1}(X - C_n) = 1$ for the cumulative probability.

For calculating the COPT it is necessary to set a certain step size. The outage capacity X is increased incrementally by this step. The size depends on the given power plant data and their classification in units. For highest accuracy, the step size should be set at least to the size of the smallest considered generation unit.

3.1.2. Residual load duration curve

A load duration curve is a load curve, where 8,760 hours of one year are sorted in descending order of their hourly load. For this thesis, hourly feed-in time series of photovoltaic and wind power electricity generation are treated as negative load. So before sorting the load, the sum of hourly photovoltaic and wind power generation time series is subtracted from the hourly load time series of Germany. The residual load time series is obtained.

If the renewable power generation in any hour is bigger than the respective load value, these hours of negative load are set to zero. If the demand of electricity can be completely met by RE sources, it is assumed that there is no risk of a loss of load in these hours. In figure 3.1 the RLDC of the year 2010 is illustrated.

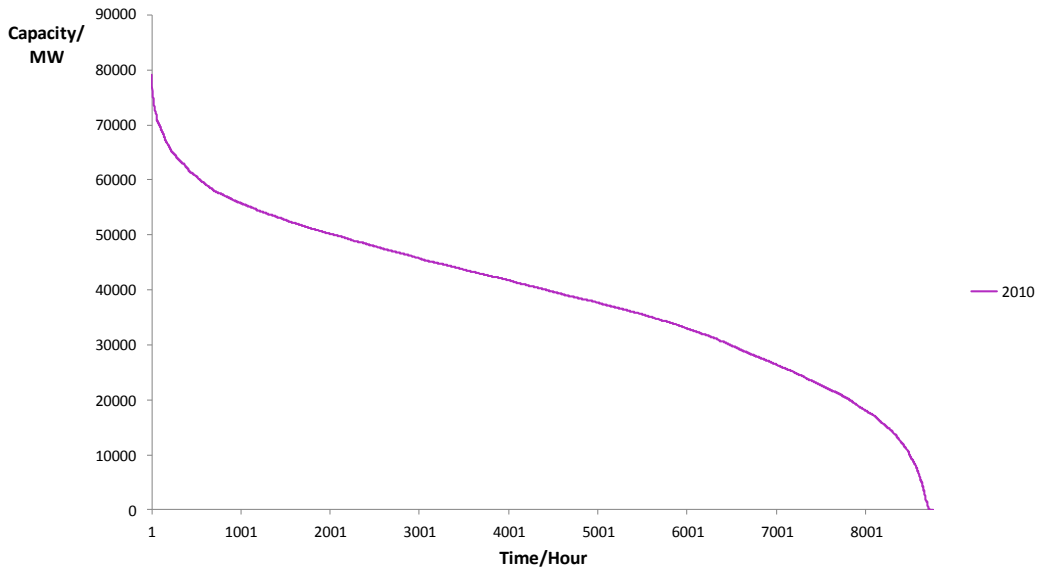


Figure 3.1.: Load duration curve 2010.

3.1.3. Loss of load expectation calculation

The LOLE is based on the probability that there will be a shortage of power, which is called the loss of load probability (LOLP). The mathematical formula for calculating LOLP is shown in equation 3.2.

$$LOLP = \sum_j P[C_A = C_j] \cdot P[L > C_j] \quad (3.2)$$

P : probability of

C_A : available generation capacity

C_j : remaining generation capacity

L : load

The remaining capacity C_j results by subtracting the outage capacity from the installed capacity. By combining the outage probability of each capacity outage state with the RLDC, the risk of a loss of load (LOLP) is obtained. This calculation process is illustrated in figure 3.2. O_j is the magnitude of the j -th outage and occurs with the probability of p_j . The probability that the load is higher than the remaining capacity ($P[L > C_j]$ of equation 3.2) is captured in t_j . This expresses the number of

days, normalized as proportion of all 8,760 hours, in which the outage would cause a loss of load in the considered energy system. The reserve of an energy system is defined by the difference between the installed capacity and the peak load. Only outage events where the outage magnitude is higher than the reserve contribute to the LOLP.

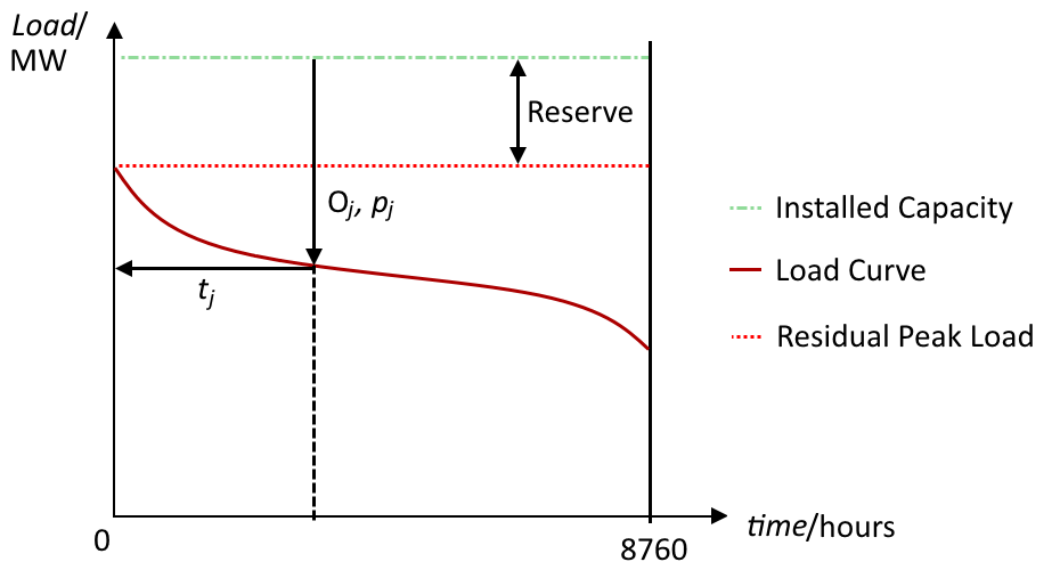


Figure 3.2.: Loss of load probability calculation.

The sum of all LOLPs is the LOLP of the considered time period shown in equation 3.3. This probability multiplied by the time T (8,760 h) is the expected number of hours in a year where available generation capacity is not meeting the demand, which gives the LOLE. This relationship is shown in equation 3.4. The LOLE calculation is implemented in Python as well and the script can be found in appendix B.

$$LOLP = \sum_j p_j \cdot t_j \quad (3.3)$$

$$LOLE = LOLP \cdot T \quad (3.4)$$

3.2. Constrained loss of load expectation

The LOLE which is calculated for determining the influence of various meteorological years on system reliability in this thesis is named constrained LOLE. Usually system reliability is calculated by using a LOLE approach for a single node power plant portfolio. However, a single node energy system is simplified and constrained in its actual flexibility. This means the calculated LOLE is only affected by the load net of the power production of FREs (residual load) and the conventional power plant portfolio.

For analyzing the sensitivity of system reliability indicator LOLE, it is important to vary only one input data, which affects the result. The focus of this thesis is on the impact of various meteorological years, which are expressed by the potential electricity generation time series of fluctuating renewable energy sources (GFRE). Thus all input data besides the generation time series of FREs remain the same for each constrained LOLE scenario. Equation 3.5 shows how the residual load time series is calculated for determining the constrained LOLE.

$$RL = L - (C_{pv} + C_w) \quad (3.5)$$

RL : residual load time series

L : load time series

C_{pv} : photovoltaic electricity generation time series

C_w : wind electricity generation time series

3.3. Correlation between meteorological years and system reliability

For an energy system, meteorological conditions have primarily influence on power generation of FRE sources. Photovoltaic and wind power have currently the highest proportion of weather depending energy sources in Germany [1]. The GFRE is obtained by summing the hourly potential electricity generation time series of photovoltaic, wind onshore and wind offshore power.

Characterization of meteorological years

Historical time series of seven years (2006 - 2012) are used to determine correlations. Meteorological years are fluctuating and patterns vary from year to year. Considering just one characteristic is insufficient for analyzing each time series. Each time series has a high resolution of hourly time steps and hence reflects weather conditions of 8,760 hours. So there are several possible indicators which capture different characteristics. For this analysis common statistical indicators are selected. On the one hand the mean, maximum and minimum values are used along with the standard deviation and the integral of the GFRE, which expresses the amount of energy generated by FRE sources. On the other hand gradients of each time series are used to capture the fluctuation of each year.

Correlation

Correlations are useful to indicate relationships between two random variables or sets of data. This statistical measure is used in this thesis to assess the relationship between characteristics of GFRE and the constrained LOLE. Pearson's correlation coefficient is used to determine correlations. Equation 3.6 is applied to calculate the correlation coefficient r [3]. For applying Pearson's correlation, both series of values need to be approximately normally distributed. This is the case for the input data of both correlated series. The GFRE, the hourly gradients and the load time series are approximately normally distributed.

$$r = \frac{\sum_{i=1}^n (x_i - \bar{x}) \cdot (y_i - \bar{y})}{\sqrt{\sum_{i=1}^n (x_i - \bar{x})^2} \sqrt{\sum_{i=1}^n (y_i - \bar{y})^2}} \quad (3.6)$$

r : correlation coefficient

x_i : annual LOLE

\bar{x} : average LOLE

y_i : annual statistical indicator

\bar{y} : average statistical indicator

3.4. Energy system model REMix

REMix is an energy system model developed and applied in several PhD thesis [16] [8] [9] [26] at the DLR. REMix uses geo-referenced meteorological data to consider spatial and temporal components of renewable power generation. One big advantage of REMix is that it considers real weather conditions. Thus correlations between electrical supply by RE sources and demand as well as heat demand are taken into account. The model uses a bottom-up approach based in linear optimization and calculates the least cost operation and expansion of a power system of a given year for countries situated in the region Europe, Middle East and North Africa (EUMENA). REMix consists of two coupled modules illustrated in figure 3.3. The resource module named Energy Data Analysis Tool (EnDAT) calculates the renewable power generation potentials and the optimization module Optimization Model (OptiMo) determines supply systems and optimal costs.

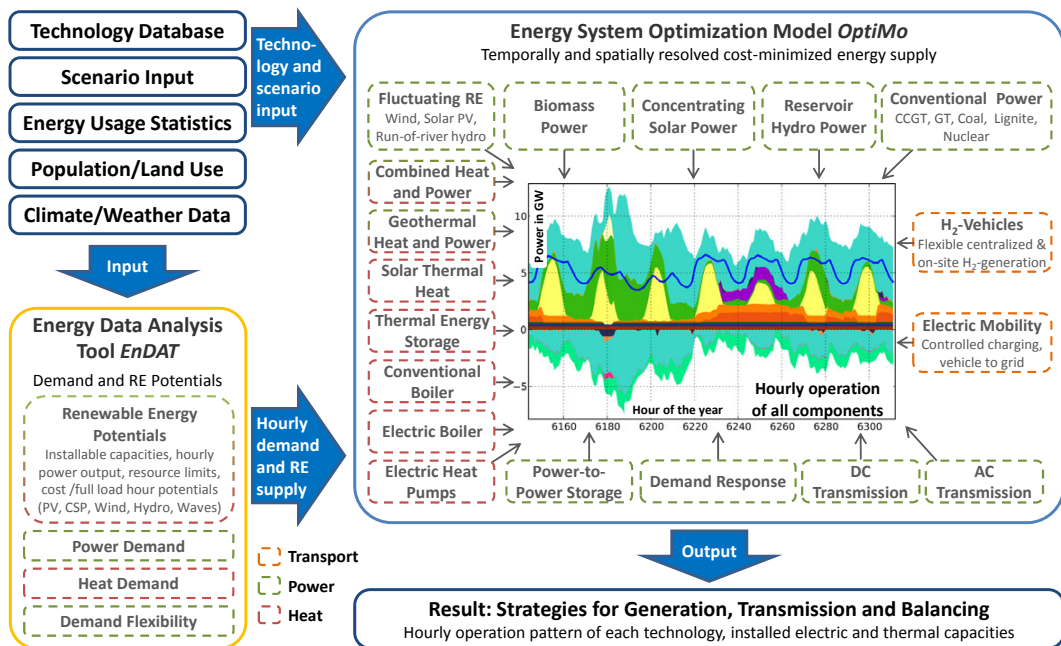


Figure 3.3.: Basic structure of the REMix model [16].

EnDAT is programmed in the C language and provides installed capacities, resource availability and hourly power output of intermittent RE sources based on geo-referenced data of land use and of meteorological phenomena. Furthermore, EnDAT delivers the biomass production potential, the inflows of hydroelectric power plants and wave power potential for each defined region. This module works on pixel-

basis, which means that for each pixel installable capacities and hourly resource data are derived.

OptiMo is implemented in the programming language GAMS, which is capable of providing a suitable environment for modeling the optimization problems. The module calculates the least cost operation and expansion that meets the heat and electricity demand. Storage as well as transmission connections between the regions enable load balancing. For optimization and border crossing exchange of electricity each region is aggregated in nodes.

3.5. Balanced loss of load expectation

Currently and even more in 2025, balancing options will be highly important for the German and the European power supply system. These balancing options are considered by applying energy system model REMix.

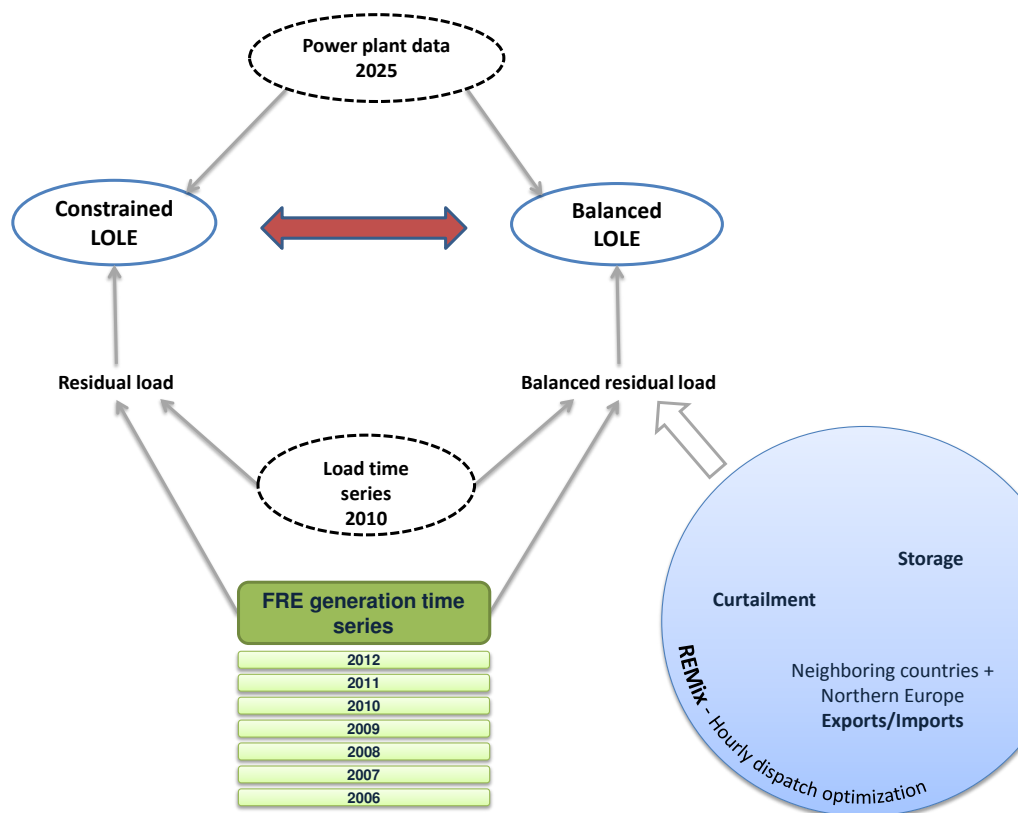


Figure 3.4.: Comparison of input data for each loss of load expectation approach.

3. Methodology

Figure 3.4 illustrates similarities and differences between the input data of the constrained and the balanced LOLE approach. Detailed input data and data sources are mentioned in the section 3.6. For obtaining the LOLE for the year 2025, different energy supply scenarios are implemented in REMix. These scenarios are based on constant input data except varying the used generation time series of photovoltaic and wind power. As mentioned in section 3.3 these time series are used to express yearly weather conditions.

The output of each REMix scenario comprises a large number of information about the calculated scenario of the year 2025. The output includes information about conventional power generation (e.g. fuel costs, generation capacities), electrical demand, each RE technology (e.g. costs, curtailed power output), storage (e.g. charged power, discharged power output) and alternating current (AC) as well as direct current (DC) transmissions (e.g. exports, imports). For calculating the balanced LOLE, all output time series which affect the load time series of Germany are selected. First of all the obtained curtailed time series of power output generated by FREs is deducted from the load. In addition this named curtailed residual load is affected by further load balancing options. On the one hand flexibility options such as storage discharge along with electricity imports reduce the load. The hourly time series of these flexibilities are subtracted from the load. On the other hand hourly time series of storage charging and electricity exports increase the load and thus are added. This curtailed residual load including flexibility options is named balanced residual load in this thesis. The determination of the balanced residual load time series is shown in equation 3.7.

The approach for calculating the balanced LOLE is methodologically equal to the calculation approach described in section 3.1. But instead of only using the residual load, the balanced residual load is used to determine system reliability for 2025. So for each considered weather year, two different LOLEs are determined and can be compared.

$$BRL = L - (C_{c,pv} + C_{c,w}) - C_{d,s} - C_i + C_{ch,s} + C_e \quad (3.7)$$

BRL : balanced residual load time series

L : load time series

$C_{c,pv}$: curtailed photovoltaic electricity generation time series

$C_{c,w}$: curtailed wind electricity generation time series

$C_{d,s}$: storage discharging time series

C_i : electricity import time series

$C_{ch,s}$: storage charging time series

C_e : electricity export time series

3.6. Used data

3.6.1. Data sources

All data sources which are used for this thesis are listed in table 3.2. External as well as internal data sources are used for calculating both LOLE approaches.

Data	Data source
Load data	ENTSO-E [11]
Plant data of installed dispatchable capacities in Germany	World Electric Power Plants Database [21]
Installed capacities CNW	DLR [2]
forced outage rates	VGB Power Tech: Bericht zur "Verfügbarkeit von Wärmekraftwerken" [14]
Renewable electricity generation potentials CNW	DLR [26]
Renewable energies installed capacities	DLR [2]

Table 3.2.: Data sources.

3.6.2. Data input

Power plant data Germany

Input data are forming the foundation for both LOLE calculations and especially for the applied REMix scenarios. The German power plant data base is shown in table 3.3. This table consists of dispatchable power plant technologies assumed for the

3. Methodology

year 2025 which are based on capacity retirement graphs depending on the World Electric Power Plants Database. As mentioned in section 3.1.1, it is necessary to use installed capacities of each technology divided in units for calculating the COPT. The German power plant data for 2025 include Biomass Power Plants (Biomass), pumped storage (PS), combined cycle gas turbine power plants (CCGT), natural gas power plants (GT-NGas), coal-fired steam turbine power plants (ST-Coal) and lignite-fired steam turbine power plants (ST-Lignite). PS is included due to the high amount of conventional power plants in the energy system. It is presumed that in case the PS is discharged (e.g. due to daily peak demand), enough conventional energy is available in the following hours to charge the storage again. As the FOR of each power plant technology is based on outage and service hours, which vary yearly, the FORs originates from a single year (2013)[14].

Technology	Unit Size (MW)	No. Of Units	FOR
Biomass	16	56	0.120
PS	239	40	0.200
CCGT	600	2	0.023
CCGT	382	16	0.023
CCGT	89	119	0.023
GT-NGas	360	2	0.023
GT-NGas	92	2	0.023
GT-NGas	11	117	0.023
ST-Coal	852	14	0.060
ST-Coal	528	4	0.060
ST-Coal	174	27	0.060
ST-Lignite	915	11	0.065
ST-Lignite	500	3	0.065
ST-Lignite	158	13	0.065

Table 3.3.: Dispatchable power plant data of Germany.

Considered regions

Among the flexibility options, export and import of electricity have a crucial role with regard to the increasing amount of border crossing grids. Figure 3.5 shows all considered countries for the balanced LOLE approach. Primarily these countries are neighboring countries of Germany plus parts of northern Europe which are connected to Germany via high-voltage DC transmission lines. These considered regions are named Central and North Europe (CNE) and includes Austria, Belgium, Czech Republic, Denmark, France, Germany, Italy, Luxemburg, Netherlands, Norway, Poland, Sweden and Switzerland. Denmark is a exceptional case because it is divided in West and East. This is due to the different regional group (RG) of syn-

chronous electrical grids [12]. Denmark East (basically the eastern islands) belongs to the RG Nordic along with Sweden, Norway and Finland, while the western part of Denmark is connected to the territory of the ENTSO-E Continental Europe RG.

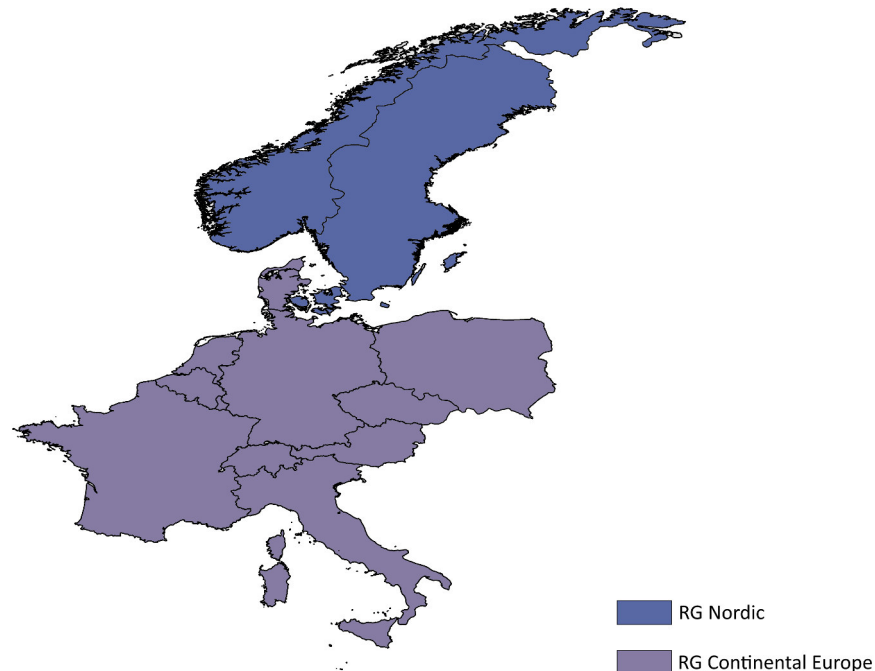


Figure 3.5.: Countries considered in the REMix scenarios applied for the balanced loss of load expectation approach.

Installed capacities in Central and North Europe

The installed capacities of the year 2025 of each country of CNE are listed in appendix C. In table C.1 the installed capacities of dispatchable power plants are listed except of PS power plants. As for PS power plants both the capacity of the installed converter and the amount of energy which can be stored is important, a separate table C.2 lists details of PS power plants in Germany. The list of the installed capacities of FRE sources, in particular wind and photovoltaic, in Europe for 2025 is shown in table C.3. Figure 3.6 illustrates the installed capacities in Germany in the year 2025.

3. Methodology

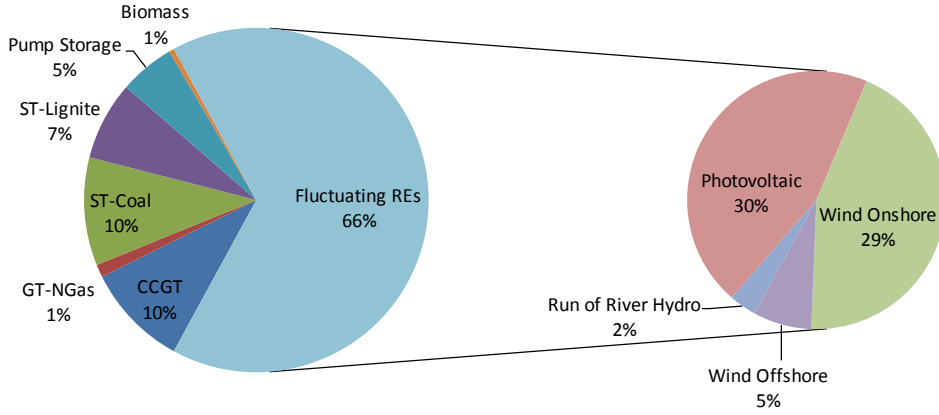


Figure 3.6.: Installed capacities in Germany in 2025 [21] [2].

Generation time series of Renewable Energy sources

Within the framework of the dissertation by Scholz [26] solar and wind electricity generation potentials of Europe and North Africa were investigated. Like the module EnDAT (mentioned in section 3.4), this investigation is based on pixel basis. The hourly time series of wind speed and solar radiation of each pixel in the investigation area is coupled with settlement areas, protected areas and infrastructure to obtain solar and wind electricity generation potentials ($P_{pot}(t)$). With these listed constraints, potential installed capacities of FREs ($P_{inst,max}$) are determined. Equation 3.8 describes how the generation time series ($P(t)$) of wind onshore, wind offshore and photovoltaic is calculated using the installed capacities of the year 2025 ($P_{inst,2025}$).

$$P(t) = \frac{P_{pot}(t)}{P_{inst,max}} \cdot P_{inst,2025} \quad (3.8)$$

$P(t)$: generation capacity

$P_{pot}(t)$: potential capacity

$P_{inst,max}$: maximal installable capacity

$P_{inst,2025}$: installed capacity of 2025

Besides wind and photovoltaic power, as noted in table C.3 in appendix C, run of river hydro (RRH) power is a FRE source as well. However the time series of RRH remains the same for each considered meteorological year in both LOLE approaches. Especially due to the inconsistency of available data for the period of 2006 - 2012, it was not possible to determine yearly time series in [26]. The used time series in this thesis was determined based on average full load hours of the years 2003, 2007 and 2010 originating from [26]. Moreover, RRH power is not as weather depending as photovoltaic or wind power and has only 4,161 MW (2 %) installed capacity in Germany in 2025 [2].

Load time series

The hourly load time series which is used in this thesis captures the electrical demand in the transmission systems. ENTSO-E notes that Germany has a comparatively high feed-in of electricity originating from RE sources into the distribution grid [12]. To capture this distribution the load time series is adjusted by the factor 1.1.

Both LOLE approaches and the included REMix scenarios are based on the same load time series of a single year. As mentioned in section 3.3 the focus of this thesis is on the weather depending generation time series of FRE sources. Thus the load time series remains the same for each investigated meteorological year. The year 2010 is chosen as load time series. It is the same year as the used technological parameters of FRE technologies in [26]. Due several year depending data in this thesis, the attempt is made to use consistent input data.

Chapter 4

Results

4.1. Analysis of individual meteorological years

In this section all seven meteorological years are characterized by several indicators. As mentioned in section 3.3 each meteorological year is expressed by hourly values of potential electricity generation of FRE sources in Germany for the period 2006 - 2012. For both LOLE approaches, the sum of photovoltaic and wind power electricity generation time series is subtracted from the load to obtain the residual load. Hence instead of characterizing the time series of photovoltaic, wind offshore and wind onshore electricity generation individually, the sum of all three time series is mostly characterized. Common statistical indicators are listed in tables and are illustrated in box plots for each year. Furthermore the amount of energy generated by FRE sources is analyzed and depicted.

4.1.1. Power generation

In table 4.1 a statistical analysis of the hourly GFRE is captured. Four indicators, all expressed in MW, characterize each year in a different way. In addition to the yearly examination, the last row notes the average of all seven years.

The hourly average mean value of potential electricity generated by photovoltaic and wind power over the whole obtained time period is 57,409 MW. One extreme value is the mean value of the year 2010 (52,975 MW), which is almost 8 % smaller than the average value. For 2007 the mean value is 60,878MW, which is 6 % greater than the average value and thus is the other extreme value. While for 2012 the mean

4. Results

Meteorological Year	Mean (MW)	Standard Deviation (MW)	Min (MW)	Max (MW)
2006	56,563	30,646	2,107	149,270
2007	60,878	31,888	2,127	156,741
2008	59,298	30,385	1,636	150,529
2009	55,636	29,108	2,419	160,656
2010	52,975	28,709	2,206	164,976
2011	59,161	30,852	1,192	147,400
2012	57,348	29,878	1,570	139,806
2006 - 2012	57,409	30,209	1,894	152,768

Table 4.1.: Characterization of the hourly potential electricity generation time series of fluctuating renewable energy sources for each meteorological year.

value (57,348 MW) is only 61 MW (0.11 %) smaller than the average value of all seven years.

The average standard deviation (STD) is 30,209 MW. In 2007 the STD was 5.6 % (1679 MW) greater than the average value. The STD for the year 2010 is 28,709 MW (about 5 % smaller than the average STD), which is smallest STD.

Besides STDs and mean values, both extreme values of each hourly time series are noted. The average minimum (1,894 MW) is only about 3 % of the average mean value while the average maximum (152,768 MW) is about 166 % greater than the average. Compared to the average maximum, the maximum value of the year 2010 is almost 8 % higher and the maximum value of 2012 about 8 % smaller. The box plot shown in figure 4.1 illustrates all listed indicators of table 4.1.

Usually a box plot graphically depicts groups of numerical data through their quartiles. In case of this thesis, box plots are used to depict STDs, mean values and maximum and minimum values. So this box plot reveals the analysis of table 4.1 at a glance. Each year is depicted along the abscissa in its own plot. The ordinate axis represents the capacity in MW. For each year the top horizontal line indicates the maximum value and the undermost horizontal line the minimum value. The rectangular box represents the STD including the mean value which divides the box in two parts of equal size.

When considering the mean values illustrated in the box plot, it can be assumed that the energy scenario using the meteorological year of 2007 has a lower LOLE than the energy scenario using 2010, since 2007 has a higher mean value. The same can be assumed for the energy scenarios using 2008 and 2009 as weather year. All scenarios using the same dispatchable generation capacity and the mean

4.1. Analysis of individual meteorological years

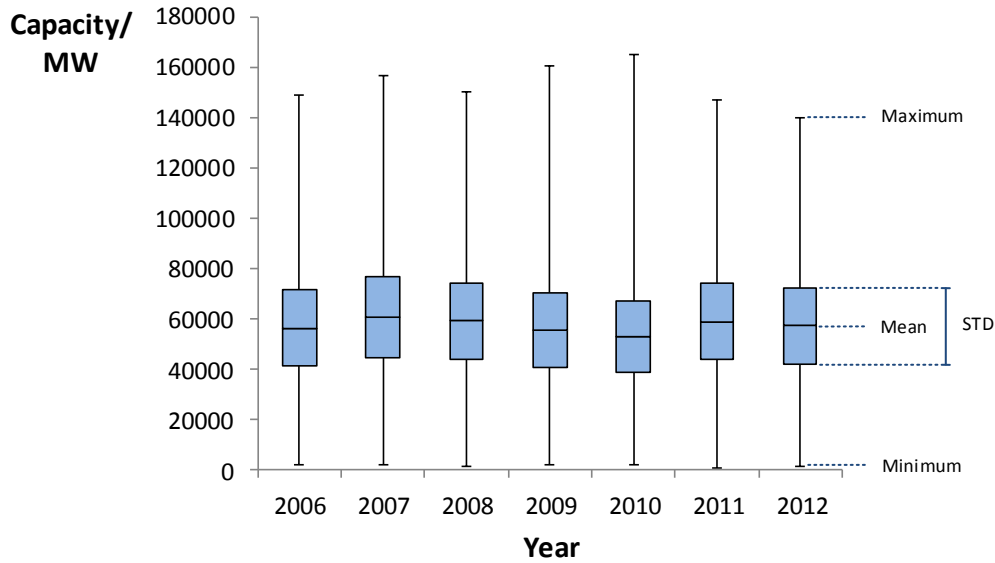


Figure 4.1.: Box plot of several indicators for characterizing the potential electricity generation time series of fluctuating renewable energy sources for each meteorological year.

hourly electricity generation of FRE sources is higher in 2008, thus a higher system reliability is supposed.

4.1.2. Annual energy

The investigations presented above analyze the hourly generated power of each considered meteorological year. In this subsection the potential amount of energy of each year is analyzed. Table 4.2 lists the annual amounts of energy in megawatt-hours (MWh) of each technology as well as the sum of all FRE.

Meteorological Year	Photovoltaic (MWh)	Wind Offshore (MWh)	Wind Offshore (MWh)	Sum (MWh)
2006	82,527,639	296,367,480	116,592,491	495,487,610
2007	79,000,263	320,183,508	134,123,438	533,307,209
2008	77,396,255	320,283,141	121,770,250	519,449,646
2009	82,164,662	299,791,182	105,412,969	487,368,813
2010	76,151,182	286,012,198	101,897,221	464,060,601
2011	83,052,564	324,620,763	110,574,962	518,248,289
2012	81,855,634	312,763,948	107,748,240	502,367,822
2006 - 2012	80,306,886	308,574,603	114,017,081	502,898,570

Table 4.2.: Amount of potential energy generated by fluctuating renewable energy sources of each meteorological year.

4. Results

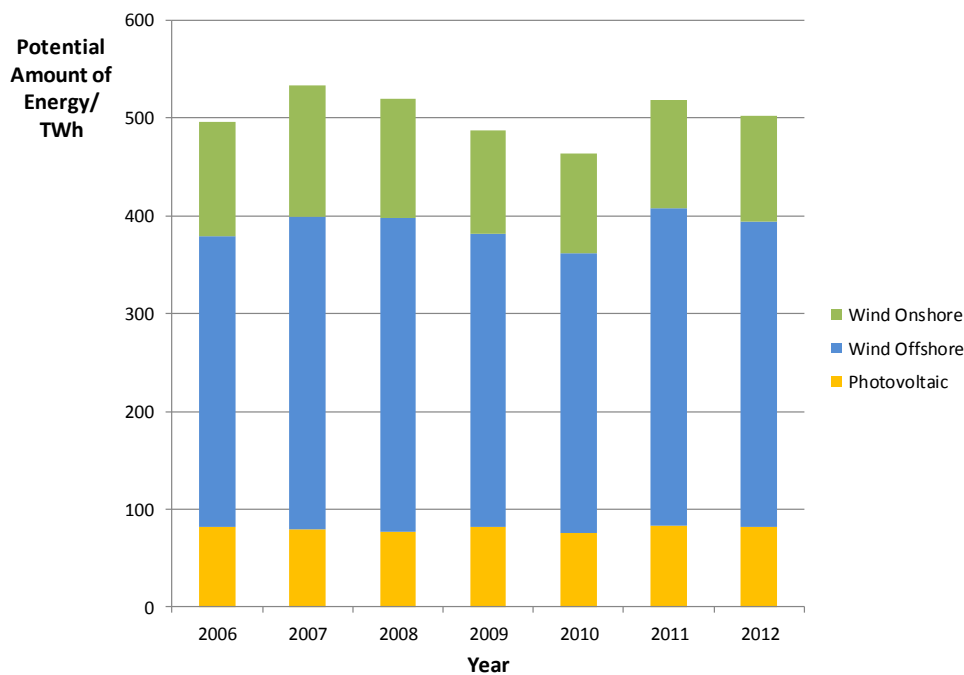


Figure 4.2.: Potential amount of energy generated by fluctuating renewable energy sources in Germany of each meteorological year.

The potential amounts of energy and the mean values, listed in table 4.1, are correlated to each other. An high annual amount of energy results a high annual mean value of the hourly GFRE. Thus the meteorological years which have the maximum, minimum and average amount of energy are the same for both indicators. Furthermore the percentage deviations correspond completely with the analysis of the mean values. The year 2007 has the maximum, 2010 the minimum potential amount of energy and the potential amount generated in 2012 is almost on average.

In addition, the differences of the potential amounts of energy of each year and the varying shares of each technology are illustrated in figure 4.2. In this plot, the ordinate axis shows the potential amount of energy in terawatts-hours (TWh) and each year is listed on the horizontal axis.

Assuming that the amount of energy generated by FRE has an essential influence on system reliability, it can be surmised that the system reliability of the scenarios using 2007 or 2008 as meteorological input year is higher than using 2010 or 2009.

4.1.3. Gradients

Hourly gradients are an approach to capture the annual fluctuation of a time series. Absolute hourly gradients describe the absolute difference between the value of the actual hour and the value of the previous hour. Performing this procedure for 8,760 hours, 8759 gradients are calculated.

The gradients are analyzed by the same statistical indicators as the actual time series of potential electricity generation and in table 4.3. This table is structured as table 4.1; the last row notes the average of all seven years for each indicator.

Meteorological Year	Mean (MW)	Standard Deviation (MW)	Min (MW)	Max (MW)
2006	3,715	3,383	0.78	40,390
2007	3,677	3,354	0.28	33,262
2008	3,566	3,310	0.39	69,127
2009	4,030	3,927	1.45	32,375
2010	3,848	4,186	0.33	43,794
2011	3,778	3,463	0.20	25,904
2012	3,770	3,409	0.34	23,958
2006 - 2012	3,769	3,576	0.54	38,402

Table 4.3.: Characterization of absolute hourly gradients of the potential electricity generation time series of fluctuating renewable energy sources for each meteorological year.

Considering the mean gradients, the average mean gradient is 3,769 MW. The year 2008 has the smallest mean gradient of 3,566 MW, which is about 5.5 % smaller than the average gradient. The time series of 2009 has the greatest mean gradient (4,030 MW). It is almost 7 % greater than the average.

The average STD of the hourly gradients for the period 2006 - 2012 is 3,576 MW. The STD of 2008 is 3,310 MW which is the smallest value of all STDs. In 2010, the STD of the hourly gradients is more than 17 % greater than the average. The closest STD to the average is reached in 2011.

The second-last column depicts the minimum value of all 8,759 gradients of each year, where all minimum gradients are in the range between 0 and 1.5 MW.

The last column notes all maximum values. The highest gradient of the last column is 69,127 MW, which is the maximum of the year 2008. It is around 80 % greater than the average maximum (38,402 MW). The time series of 2012 contains a maximum gradient of 23,958 MW, which is almost three times smaller than maximum gradient of 2008.

4. Results

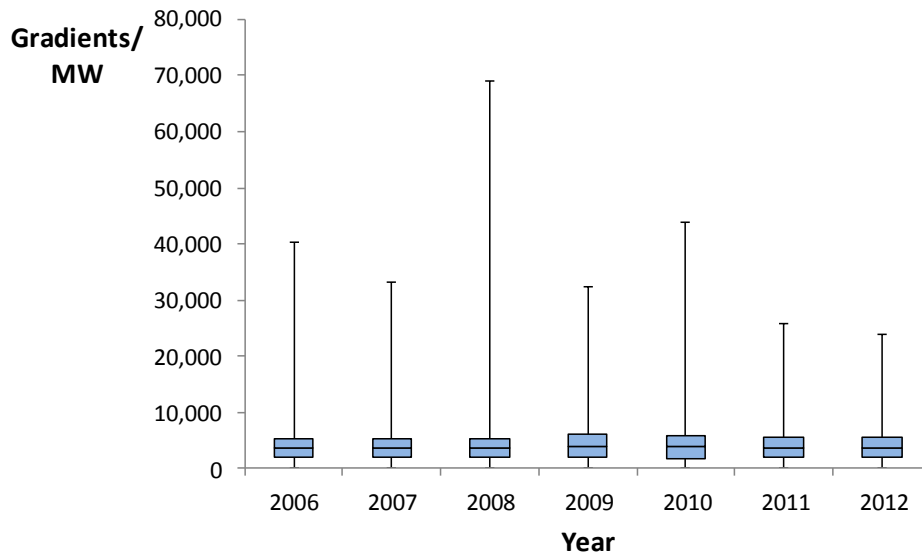


Figure 4.3.: Box plot of several indicators for characterizing the hourly gradients of the potential electricity generation time series of fluctuating renewable energy sources for each meteorological year.

Instead of analyzing table 4.3, the extreme values of every indicator can be read out of figure 4.3. This box plot illustrates the indicators listed in table 4.3. It can be seen that GFRE of 2009 has a higher mean gradient than the year 2008. Which means that the hourly annual fluctuation in 2009 is higher and thus it can be assumed that the LOLE of this scenario is higher than that of 2008.

4.2. Analysis of the time period 2006 - 2012

4.2.1. Annual energy

Each determined statistical indicator of the GFRE, listed in section 4.1 can be discussed in its own way. The maximum and the minimum values just give margins of the obtained sets of data. Analyzing the maximum or the minimum value just considers one of 8,760 values, while the mean value and the annual amount of energy captures all 8,760 values. So for an annual comparison, which is done in this thesis, mean values and the potential amounts of energy have a greater importance. The potential amounts of energy express how much electrical energy could potentially be transformed from photovoltaic and wind power in a specific year. As mentioned

in section 4.1 above, it is assumed that this value has a significant influence on the constrained LOLE.

By analyzing the yearly variation of the potential amounts of energy, the STD is a valuable measure. The STD of all seven years, shown in table 4.2 before, is 21,511 gigawatt-hours (GWh), which is only about 4.3 % of the average amount of energy. Hence the STD is relatively small and therefore implies a low annual variation compared to the 502,899 GWh which are yearly generated by FRE on average.

An in-depth analysis of the potential amount of energy where each FRE source is considered separately reveals that wind offshore as well as wind onshore power has a greater contribution to the annual fluctuation as shown in figure 4.2. A better evidence for that statement is obtained by considering the standard deviation of the potential numbers of full load hours of each technology over the seven considered years. The full load hours are determined by dividing the potential amount of energy of each technology by the maximum potential installed capacity, which remains the same for each year. Table 4.4 lists the potential numbers of full load hours of each technology as well as the standard deviation.

Meteorological Year	Photovoltaic (h)	Wind Offshore (h)	Wind Onshore (h)
2006	883	4,118	2,105
2007	845	4,449	2,421
2008	828	4,451	2,198
2009	879	4,166	1,903
2010	814	3,974	1,840
2011	888	4,511	1,996
2012	875	4,346	1,945
Standard Deviation	27	188	186

Table 4.4.: Potential number of full load hours of each technology of each meteorological year.

The STDs of the potential numbers of full load hours of wind onshore (186 hours) and wind offshore (188 hours) have almost the same fluctuation during the period of seven years. In contrast, considering the STD of photovoltaic power, this STD is almost seven times less than the STD of wind power, which means the fluctuation of wind power is significantly higher from year to year than the fluctuation of photovoltaic power.

4. Results

4.2.2. Gradients

Besides considering the annual variations of the amounts of energy, the gradients of the GFRE give evidence concerning the fluctuation of each meteorological year. A high mean gradient implies a higher hourly difference and thus a higher annual fluctuation. The average absolute hourly mean gradient, which is listed in table 4.3 is around 3.8 gigawatts (GW). These are about 7 % of the average hourly mean value of the GFRE and indicates a high annual fluctuation.

The STD of the mean gradients give evidence of the fluctuation of all seven years. The hourly mean gradients have a yearly fluctuation of about 135 MW, which is only around 3.6 % of the average mean gradient. This indicates a weak fluctuation during the period of 2006 - 2012.

Meteorological Year	Photovoltaic (%)	Wind Offshore (%)	Wind Onshore (%)
2006	2.64	2.43	1.50
2007	2.53	2.56	1.58
2008	2.44	2.46	1.49
2009	2.85	2.66	1.46
2010	2.77	2.55	1.31
2011	2.65	2.43	1.41
2012	2.56	2.64	1.48
2006 - 2012	2.63	2.53	1.46

Table 4.5.: Normalized hourly mean gradients of the potential electricity generation time series of each technology of each meteorological year.

Here again, if the hourly gradients of each technology are analyzed, more differences can be determined. The average normalized gradients for photovoltaic (2.63 %) and wind offshore (2.53 %) are about the same value of 2.5 %, while the average normalized gradient for wind onshore is only about 1.5 % (shown in table 4.5). That means that the mean hourly differences for wind onshore power are about 60 % smaller. Thus hourly electricity generated by photovoltaic and wind offshore power fluctuate more than wind onshore power.

In addition to these values, the frequency distribution of the hourly normalized gradients of the potential electricity generation time series of each FRE source is illustrated and can be found in figures 4.4 - 4.6. The x-axis depicts the normalized hourly gradients while the vertical axis shows the frequency distribution.

The time series of the year 2011 is chosen to illustrate different distributions. If comparing the frequency distribution of wind offshore (figure 4.5) and photovoltaic (figure 4.4), both plots are relatively dissimilar in their shapes. The frequency of

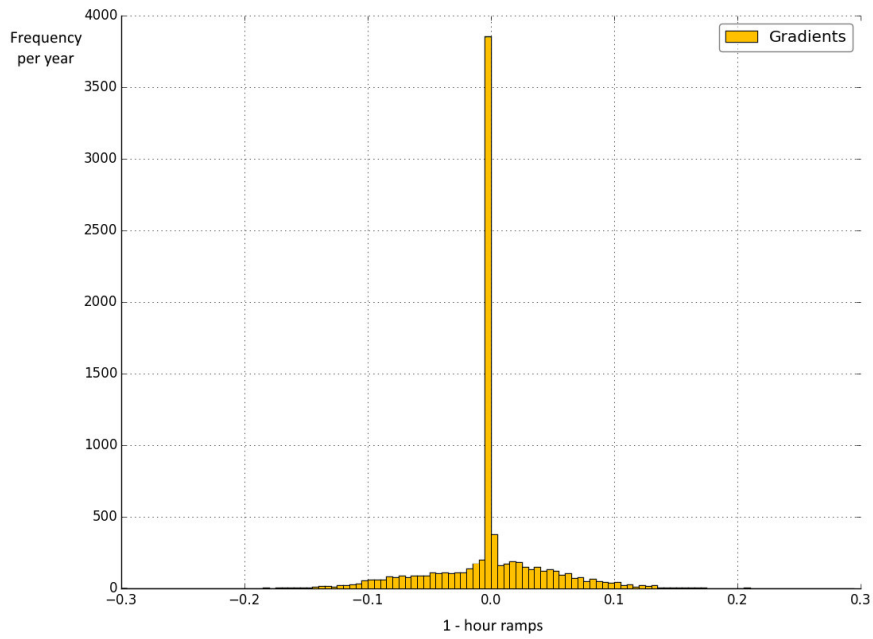


Figure 4.4.: Frequency distribution of absolute hourly gradients of the potential electricity generation time series of photovoltaic power 2011.

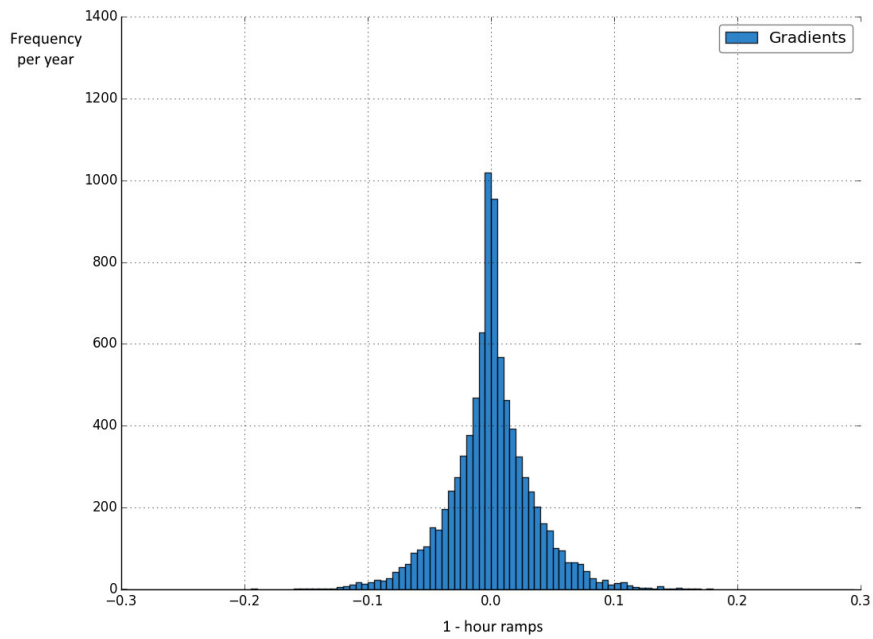


Figure 4.5.: Frequency distribution of absolute hourly gradients of the potential electricity generation time series of wind offshore power 2011.

4. Results

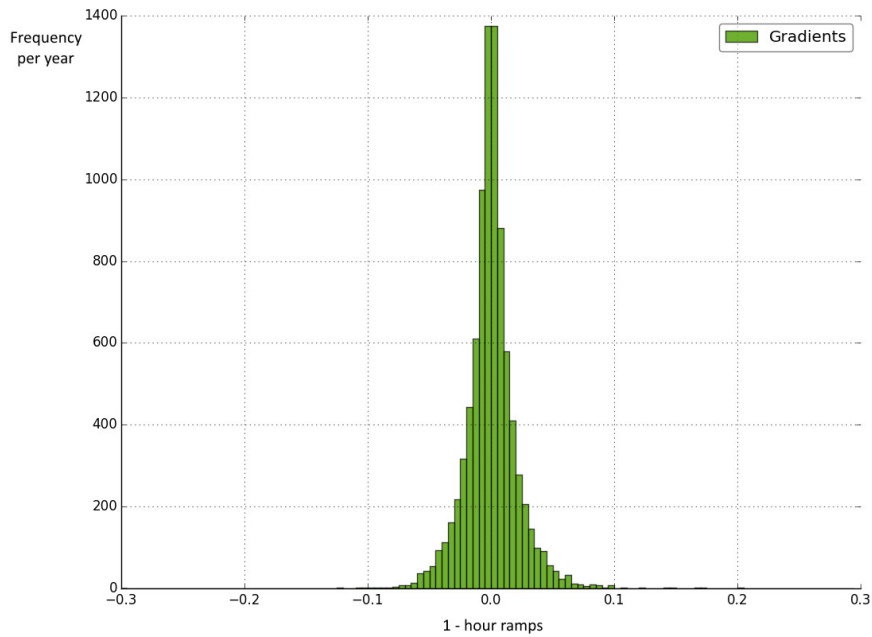


Figure 4.6.: Frequency distribution of absolute hourly gradients of the potential electricity generation time series of wind onshore power 2011.

normalized gradients of photovoltaic is close to zero extremely high, due to the day-night cycle. But on average both technologies have an almost equal average mean gradient. On the other hand, the shape of the distribution of hourly gradients of the wind onshore generation time series (figure 4.6) is quite similar to the distribution of wind offshore. However the frequency for hourly ramps in the range of -0.05 and 0.05 is significantly higher. Due to that, the average mean gradient (listed in table 4.5) of wind onshore is smaller.

As mentioned in chapter 3, the constrained LOLE is affected by the sum of electricity generation by photovoltaic and wind power, thus the sum of electricity generated by all three technologies need to be considered. The average normalized gradient for all three FRE sources is about 1.71 %. The frequency distribution is illustrated in figure 4.7. This figure shows that the distribution of photovoltaic is widening the distribution shapes of wind offshore and onshore.

4.3. Constrained loss of load expectation for 2025

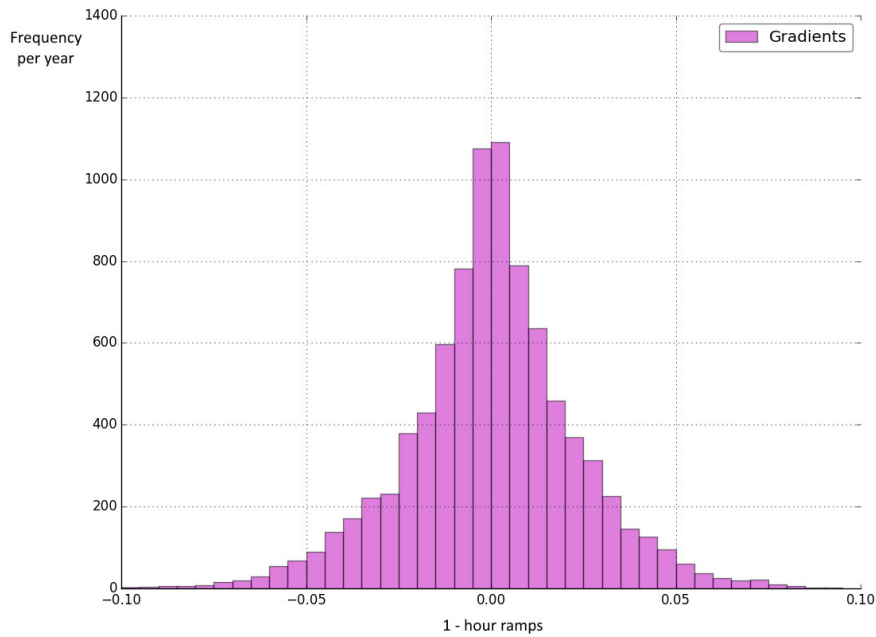


Figure 4.7.: Frequency distribution of absolute hourly gradients of the potential electricity generation time series of fluctuating renewable energy sources 2011.

4.3. Constrained loss of load expectation for 2025

In this section the results of calculating the constrained LOLE for 2025 for each meteorological year are examined. The LOLEs are obtained by applying the constrained LOLE approach described in chapter 3. Table 4.6 notes the computed LOLE for each year.

Meteorological Year	Constrained LOLE in hours/year
2006	50.98
2007	42.98
2008	44.31
2009	60.55
2010	66.75
2011	50.08
2012	60.29
2006 - 2012	53.71

Table 4.6.: Constrained loss of load expectation for 2025 of each meteorological year.

The average constrained LOLE for 2025 is 53.71 hours per year. The lowest LOLE is determined by using 2007 as meteorological year. The expectation of 42.98 hours per year is almost 18 % smaller than the average LOLE. Besides that, the delta

4. Results

between the highest LOLE, calculated using 2010 as weather year, and the lowest LOLE is 23.77 hours, which are 44 % of the average LOLE for 2025. This highest LOLE of 66.75 hours per year is more than 12 % higher than the average.

Referring to [7], no constrained LOLE for 2025 is less than the industry standard of 2.4 hours per year. Thus the used constrained energy scenario for 2025 is not reliable. It can be assumed, that due to the balancing options, the LOLE is reduced to an expectation below 2.4 hours.

The STD over all seven determined LOLEs is about 8.3 hours. Compared to the average LOLE, 8.3 hours correspond to 15.5 %. These differences are only caused by changing the input time series of the FRE sources.

Table 4.6 is analyzed in the following to verify the assumptions of the subsections above. As assumed in subsection 4.1.1 and 4.1.2, it is confirmed that the energy scenario using weather year 2007 or 2008 have a lower LOLE than using 2010 or 2009. In addition, this result confirms the supposition which is made considering the mean gradients in subsection 4.1.3 – the constrained LOLE using the GFRE of 2009 is higher than that of 2008.

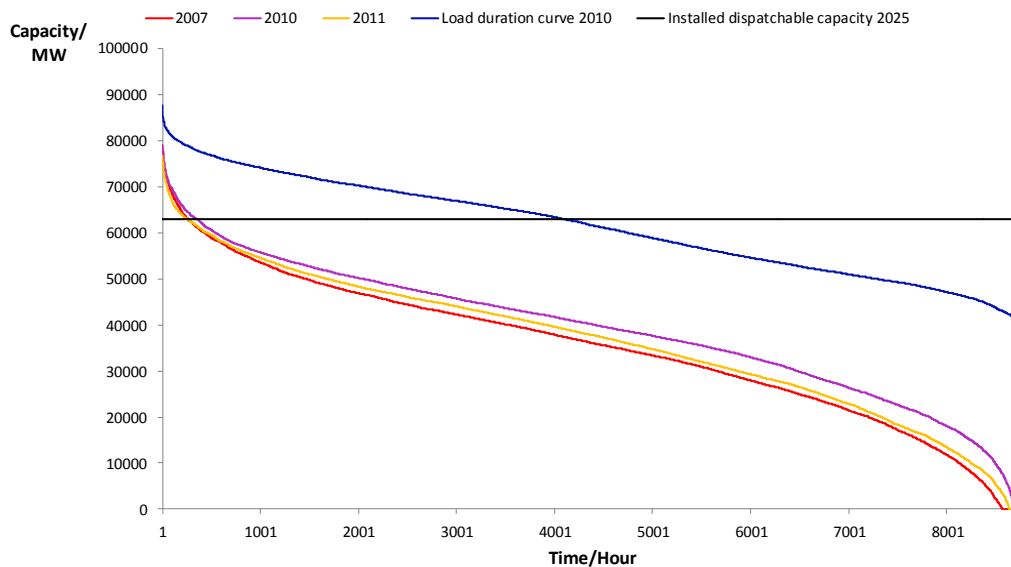


Figure 4.8.: Residual load duration curves, load curve and installed capacity used for calculating the constrained loss of load expectation.

To illustrate the differences between the maximum and minimum LOLE, figure 4.8 shows the RLDCs of the meteorological weather years 2007, 2010 and 2011. The x-axis shows the time while the vertical axis depicts the generation capacity in MW.

4.4. Balanced loss of load expectation for 2025

It can be seen that the RLDC of 2010 is the highest, followed by 2011 (average), while the RLDC of 2007 is the lowest. A high RLDC indicates a low amount of energy generated by FRE in that year and thus also a lower annual mean value of hourly electricity generation. The black line expresses the installed dispatchable capacity of Germany in 2025 and the blue curve is the load duration curve of 2010. It can be seen that the high residual load hours of all three RLDC lie above the value of installed dispatchable capacity. The assumption can be made, that by using the balanced LOLE approach, these high load hours are reduced due to balancing options. Thus the average resulting balanced LOLE is presumed to be lower than the average constrained LOLE.

4.4. Balanced loss of load expectation for 2025

Table 4.7 shows the results for the balanced LOLE approach. In contrast to the constrained LOLE, the balanced LOLE approach considers curtailment of photovoltaic and wind feed-in as well as other flexibility options, which allow spatial and temporal decoupling of generation and load. The average balanced LOLE is 0.0135 hours per year, which are around 0.8 minutes per year. No determined balanced LOLE is higher than 3 minutes (0.05 hours). A LOLE of 0.0486 minutes per year is the maximum expectation, obtained by using 2009 as input weather year. The lowest expectation (0.0037 hours/year) is computed for the balanced LOLE using weather year 2011.

Meteorological Year	Balanced LOLE in hours/year
2006	0.0070
2007	0.0071
2008	0.0151
2009	0.0486
2010	0.0079
2011	0.0037
2012	0.0048
2006 - 2012	0.0135

Table 4.7.: Balanced loss of load expectation for 2025 of each meteorological year.

The calculated balanced LOLEs confirm the presumption, that due to hourly dispatch optimization, the LOLEs are reduced below 2.4 hours per year. Thus each

4. Results

LOLE is clearly below that measure, one can state, as expressed in [7], that all seven energy scenarios including balancing options are system reliable.

The highest balanced LOLE is 3.6 times higher than the average balanced LOLE. Except of the balanced LOLE using 2008 (0.0151 hours) and 2009 (0.0486), all expectations are below 0.008. The STD of all seven balanced LOLEs is 0.0147 hours, which correspond to 109.5 % of the average balanced LOLE. As mentioned in section 4.2, the fluctuation of both, the hourly mean gradients and the amounts of energy from year to year are relative low. Due to the difference between these low fluctuations and the high inconsistent annual variation in LOLEs, it is assumed that the correlations between the balanced LOLEs and the GFRE are weak.

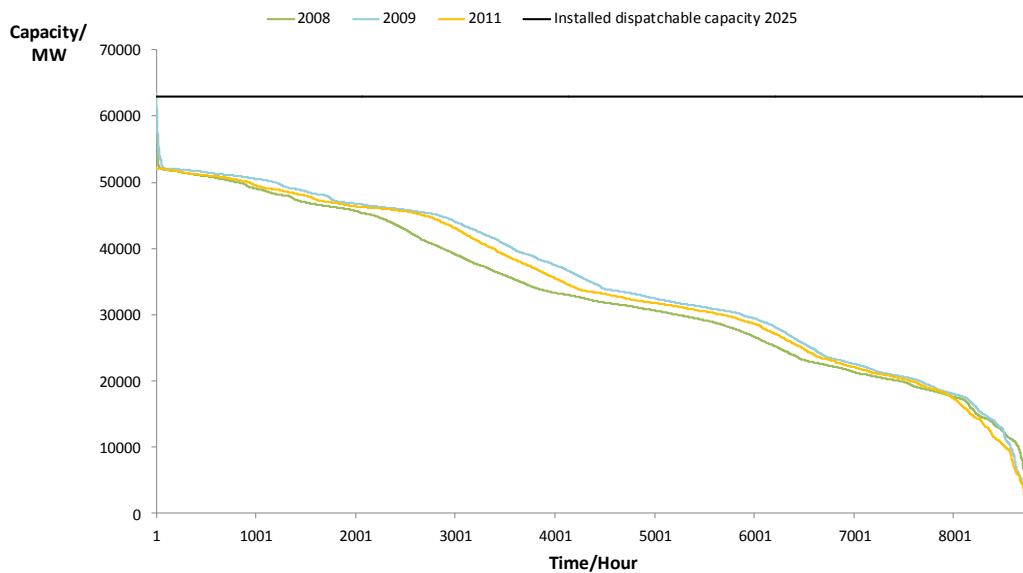


Figure 4.9.: Balanced residual load duration curves, load curve and installed capacity used for calculating the balanced loss of load expectation.

Figure 4.9 illustrates the balanced RLDC of the highest (2009), lowest (2011) and the average (2008) determined balanced LOLE. Here again, the horizontal axis shows the time, while the y-axis depicts the generation capacity in MW. The assumption, which is made section 4.3 can be confirmed. Both, the average balanced LOLE is lower than the average constrained LOLE and the balanced RLDCs are almost all below the value of installed dispatchable capacity.

Furthermore, it can be seen that the RLDC of 2009 is the highest curve. This means, that in 2009 less load hours are balanced (especially reduced) by hourly dispatch optimization. Considering the balanced RLDC of 2008 and 2011; even though the

4.4. Balanced loss of load expectation for 2025

RLDC of 2008 is lower than 2011 in the range of the 1,000th to almost the 8,000th hour, the balanced LOLE using the meteorological year of 2011 is the lowest computed LOLE. The reason for this lies in the first and thus highest balanced residual load hours. To analyze these hours, figure 4.10 plots the highest 40 residual load hours of all three mentioned balanced RLDCs.

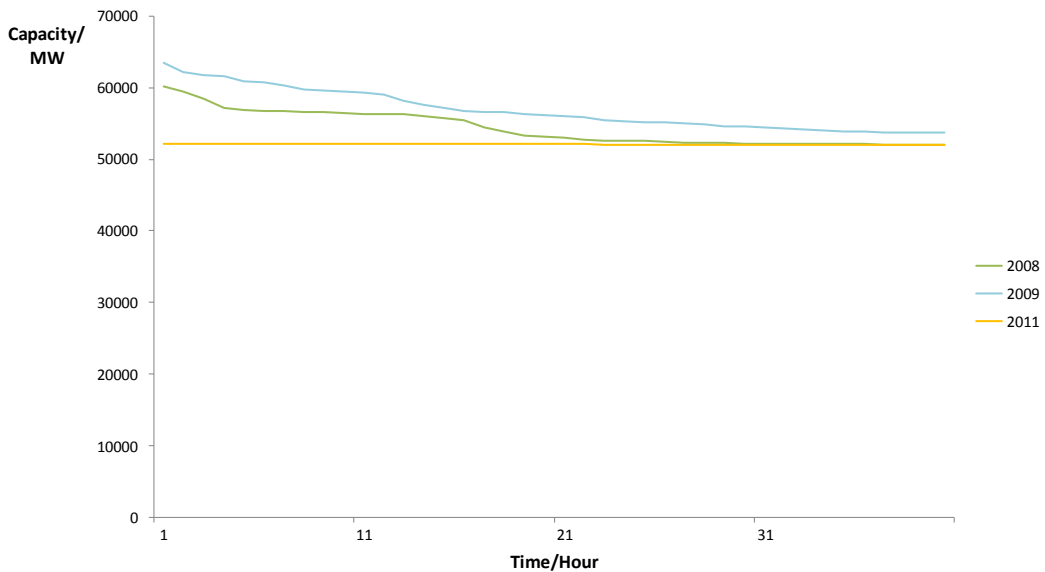


Figure 4.10.: Balanced residual load duration curves of the first 40 hours.

It is shown that the balanced residual load of 2011 has a generation capacity value of around 52,000 MW during the highest hour. From there on, the RLDC is barely decreasing. The RLDC of 2008 starts at around 60,000 MW and decreases to about the same generation capacity level than the RLDC of 2011 (52,000 MW) by the 40th hour. So one can conclude, that the reason for the lowest balanced LOLE – the hourly dispatch optimization balances even the high load hours of the German energy scenario for 2025 using weather year 2011. In contrast, the balanced RLDC of the scenario using 2008 still contains a few high load hours. The reason why high residual load hours lead to a higher LOLE is analyzed in section 4.5.

4.5. Correlation between meteorological years and system reliability

As mentioned in chapter 3.3, a correlation describes the relationship between two random variables. In this subsection, the correlations between each indicator of GFRE of all considered years and the results of the both LOLE approaches are examined. By analyzing the correlation with the constrained LOLE, the contextual connections, which are made in the subsection 4.3 are verified again and are reformulated in certain statements of a general nature. In addition, the correlation between the statistical indicators of the GFRE and the balanced LOLE is determined and analyzed.

The correlation coefficient indicates if there is a linear relationship. If the correlation coefficient is +1, there is a full positive correlation, -1 indicates a full negative correlation and the correlation coefficient 0 indicates, that there is no linear relationship.

The extreme values (maximum and minimum values) of the GFRE are not taken into account for analyzing the correlation with the system reliability. For calculating LOLEs, the whole time series of 8,760 hours is considered, thus outliers have only a low influence.

4.5.1. Constrained loss of load expectation

The results of the correlation analysis between the constrained LOLE and the statistical indicators of the GFRE are shown in table 4.8. This table contains of correlation coefficients of analyzing correlations between the hourly GFRE and the constrained LOLEs.

Statistical indicator	Correlation coefficients	
	Potential power generation	Gradients
Annual sum	-0.91	
Mean value	-0.91	0.74
Min value	0.32	0.29
Max value	0.29	-0.31

Table 4.8.: Correlation between the potential electricity generation time series of fluctuating renewable energy sources and the constrained loss of load expectation for 2025.

The first value expresses the correlation between the annual sums (amounts of energy) of the GFRE and the constrained LOLEs. The correlation coefficient is -0.91

4.5. Correlation between meteorological years and system reliability

and indicates an almost full negative correlation. The correlation between the mean values and the constrained LOLEs is also highly negative (-0.91). As mentioned in section 4.1.2, the mean values and the potential amount of energy have a full positive correlation, thus both correlation coefficients are the same.

The almost full negative correlation of the mean values and the annual amounts of energy indicate that high mean values as well as high amounts of energy result in low constrained LOLEs. This correlation verifies the contextual connections which are made in section 4.3 and furthermore states a general connection between the mean values as well as the annual sum and the constrained LOLEs.

Table 4.8 also shows the correlation between the hourly gradients of the GFRE and the constrained LOLEs. A correlation coefficient of 0.74 expresses a high positive correlation. This correlation coefficient also confirms the contextual connections which are made in section 4.3 concerning the mean gradients of the GFRE. An high LOLE is determined by using a meteorological year with a high annual mean gradient. So a coefficient of 0.74 states a general linear relationship between the constrained LOLE and the annual hourly fluctuation, expressed by the hourly mean gradient.

4.5.2. Balanced loss of load expectation

Table 4.9 shows the correlation coefficients determined by correlating the GFRE with the balanced LOLEs. The annual amounts of energy as well as the mean values of the GFRE and the balanced LOLEs have a correlation of -0.27. This expresses a weak negative correlation and confirms the assumption of section 4.4.

Considering the hourly mean gradients, a correlation coefficient of 0.66 expresses a positive correlation. That means a meteorological year, with high hourly mean gradients results in a high balanced LOLE.

Statistical indicator	Correlation coefficients	
	Potential power generation	Gradients
Annual sum	-0.27	
Mean value	-0.27	0.66
Min value	0.56	0.90
Max value	0.45	0.05

Table 4.9.: Correlation between the potential electricity generation time series of fluctuating renewable energy sources and the balanced loss of load expectation for 2025.

4.6. Discussion

4.6.1. Influence of meteorological years on system reliability

As mentioned above, the determined LOLEs for 2025 vary from year to year. Section 4.5 mentions the outcome of analyzing the relationship between the GFRE and the both LOLE approaches. This outcome is discussed in the following.

Annual energy

The correlation coefficient (-0.91) between the constrained LOLEs and the potential amounts of energy is almost full negative (subsection 4.3). This implies a negative linear relationship, which means, using a meteorological year with a high potential amount of energy, a low LOLE is expected. In other words, the smaller the yearly amount of energy, the higher the expectation that the load cannot be met.

The correlation coefficient (-0.27) determined between the balanced LOLEs (section 4.4) and the potential amounts of energy indicates only a weak negative correlation. So both correlation coefficients are negative, thus for both correlations one can conclude that a year with a high amount of energy results in a low LOLE. However, the correlation coefficient of the balanced LOLE is more than 3 times lower. This reduction of the correlation is obtained due to the application of energy system model REMix.

Analyzing the reasons for this negative correlation, one must consider the lack of energy in years with a smaller amounts of energy generated by FRE sources. As mentioned in subsection 4.2, the annual amount of energy is varying and need to be compensated by conventional or at least dispatchable power plants. Therefore the probability increases that power plants are on outage and thus the LOLE for that given year increases as well. In detail, a lower annual amount of energy generated by FRE sources lead to higher RLDC. This induces, that less capacity need to be on outage to lead to a loss of load event. A low outage capacity has a higher outage probability and thus a higher LOLE is obtained. Load balancing is reason for the differences in the correlation coefficients between both LOLE approaches. The causes are evaluated in subsection 4.6.2.

Gradients

The second correlation is investigated between the constrained LOLE and the hourly gradients of the GFRE. As shown in subsections 4.3 and 4.4, the correlation coefficients amount to positive correlations, which implies that using a meteorological year with higher mean gradients as input for both LOLE approaches, higher LOLEs are determined. As the gradients measure the fluctuation of a meteorological year, one can conclude that input time series with a higher mean hourly fluctuation lead to a higher number of expected hours in which the load cannot be met. Comparing the correlation coefficients of both LOLE approaches, the coefficient of the balanced LOLE (0.66) is slightly lower than that of the constrained LOLE (0.74). Here again, this difference is obtained due to applying energy system model REMix. The causes of the difference are analyzed in section 4.6.2.

Considering both, the correlation with the hourly gradients and with the annual amount of energy, it is to note, that the constrained LOLE is strongly correlating with the annual amount of energy, while the correlation with the hourly fluctuation, in particular the gradients, is less. On the other hand, the balanced LOLE weakly correlates with the annual energy but shows a stronger correlation with the hourly gradients. Thus it can be concluded, that balancing options partly compensate the fluctuation of annual amounts of energy generated by FRE, however, barely compensate annual hourly fluctuations.

As mentioned in section 4.3, the constrained LOLE fluctuates about 15.5 % over the considered seven years compared to the average constrained LOLE. In contrast to that, the balanced LOLE varies about 109.5 %. That is significantly more than the system reliability of a constrained German energy system. For both LOLE approaches, the same GFRE is used as input, and thus a delta of 94 % is determined comparing both fluctuations. The GFRE is analyzed over the time period of 2006 - 2012 in section 4.2 and the outcome reveals, that the annual amount of energy varies about 4.3 % and the hourly mean gradients about 3.6 % of the average values. It can thus be assumed that the balancing options are the reason for the high fluctuation of the balanced LOLEs.

4. Results

4.6.2. The impact of load balancing on system reliability

In this subsection, the impact of load balancing is analyzed and discussed. The impact is captured by comparing the results of the constrained LOLE and the balanced LOLE for 2025, which are both listed again in table 4.10.

Meteorological Year	Constrained LOLE in hours/year	Balanced LOLE in hours/year
2006	50.98	0.0070
2007	42.98	0.0071
2008	44.31	0.0151
2009	60.55	0.0486
2010	66.75	0.0079
2011	50.08	0.0037
2012	60.29	0.0048
2006 - 2012	53.71	0.0135

Table 4.10.: Constrained and balanced loss of load expectation for 2025 of each meteorological year.

Considering the average expectation of each LOLE approach, a significant difference can be observed. The average constrained LOLE is about 54 hours, while the average balanced LOLE is about 0.8 minutes (0.0135 hours) per year. So by considering flexibility options and curtailment the LOLE for the examined German energy scenario for 2025 can be nearly reduced to zero.

The calculated correlation coefficient between the constrained LOLEs and the balanced LOLE value is about 0.25. This weak correlation implies that there a low linear relationship. Thus both LOLE approaches uses the same GFRE and only differ in the fact, that the balanced LOLE considers balancing options, the low coefficient indicates the large influence of the hourly dispatch optimization.

To analyze the reasons for these clear differences, the balanced LOLE for 2025 using the meteorological year of 2011 as input is investigated in detail. 2011 is chosen, since the balanced LOLE of this scenario is lowest calculated LOLE and as mentioned in 4.4, the balanced RLDC of 2011 is highly influenced by hourly dispatch optimization.

As mentioned in chapter 3, both LOLE approaches use different RLDCs. In figure 4.11 the RLDCs of the constrained and balanced LOLE approach are illustrated along with the installed dispatchable capacity for 2025.

The balanced RLDC includes curtailment of hourly power output generated by FRE sources as well as all flexibility options. It can be seen, that the balanced residual load curve is lower than the residual load of the constrained LOLE. Especially hours

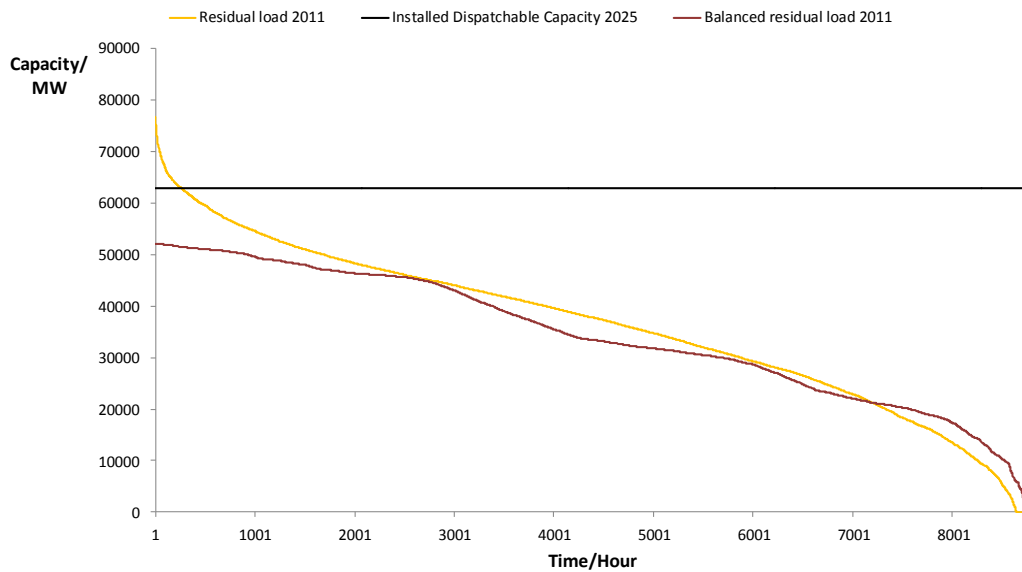


Figure 4.11.: Residual load duration curves, load curve and installed capacity used for calculating the both loss of load expectations.

of peak demand are reduced by applying the balanced LOLE approach. That can be seen by comparing both RLDCs in the range of the first to the 1,000th hour. The balanced RLDC decreases slowly from about 52,000 to 50,000 MW (delta of 2,000 MW), while the RLDC of the constrained LOLE decreases about a delta of 22,000 MW in the same time.

As a result of the lower balanced residual load curve, the integral of this curve is smaller, thus a smaller amount of energy need to be covered by conventional dispatchable energy sources. This means, a higher RLDC causes a higher LOLE.

To get more into detail, two random days in both, summer and winter are picked to point out the hourly impact of load balancing. Figure 4.12 shows May 24 and 25, while figure 4.13 depicts December 20 and 21 of 2025 using the meteorological year of 2011. In both plots the x-axis displays the time (date and hour) and the vertical axis the generation capacity in Germany in MW. The green bars represent the hourly feed-in of FRE which is the same as used for the constrained LOLE approach. The colored bars illustrate the various flexibility options. Storage charging, curtailment as well as electricity export (captured in transmission) are shown as negative capacity. The black line indicates the load. The gap between the bars and the load implies the capacity which needs to be hourly covered by dispatchable power plants for meeting the load.

4. Results

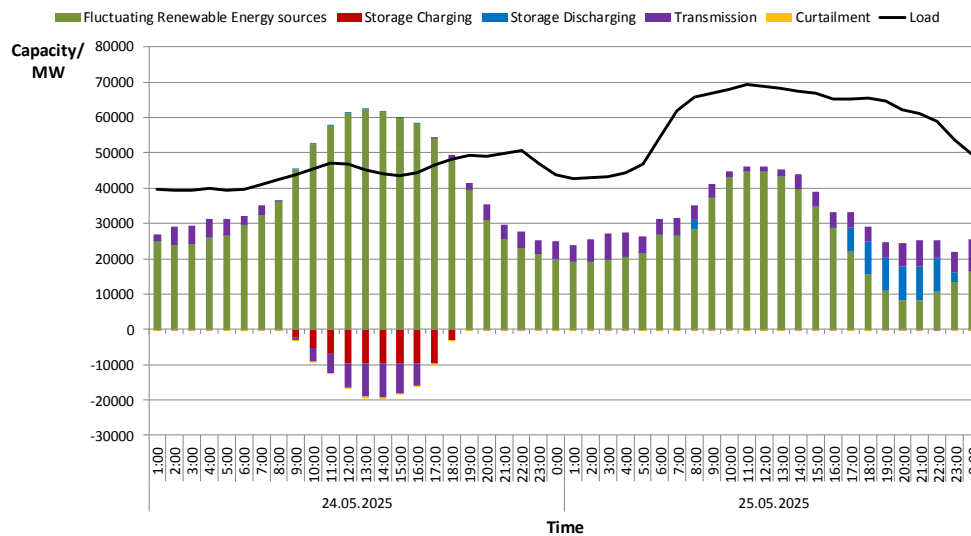


Figure 4.12.: Hourly dispatch of certain technologies for Germany on 24 and 25 May 2025 – Constrained LOLE: Power generation from FRE (only green bars), Balanced LOLE: Power generation from FRE and flexibility options (all colored bars).

Considering the two days in summer (figure 4.12), a relative high contribution of transmission can be found. Transmission includes electricity exports as well as imports. In nearly each hour of all 48 hours, Germany is either exporting or importing electricity. On May 24th, from 9 in the morning until 6 o'clock in the evening, the power generation by FRE exceeds the load. During that period, the solar radiation is decisively high and flexibility options intervene in form of storage charging and electricity export as well as curtailment of FRE feed-in. The charged storage are discharged again on the next day to balance a period of weak electricity generation of FRE in the evening.

For December 20 and 21 (figure 4.13), flexibility options have a major impact on the electric power supply as well. As the purple bars indicate, in each hour, cross-border transmissions affect the energy supply. Furthermore, storage are charged in periods of weak demand (during the night) and in periods in which dispatchable power plants are not shut down due to economic reasons, even though the demand is already satisfied. Storage are discharged again in periods of peak demand. Compared to days in the summer period, solar radiation is low in the winter months, thus no peaks of the hourly feed-in of FRE (green bars) can be noticed.

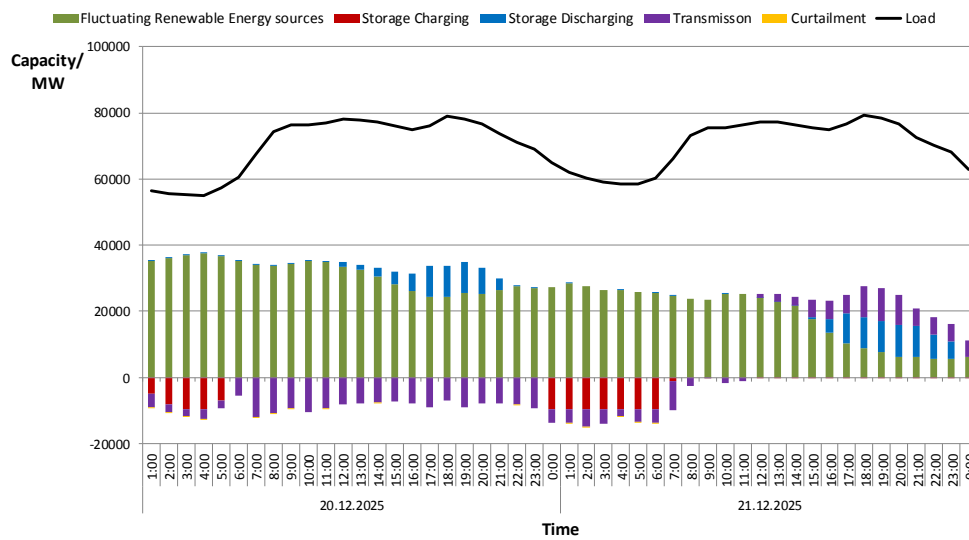


Figure 4.13.: Hourly dispatch of certain technologies for Germany on 20 and 21 December 2025 – Constrained LOLE: Power generation from FRE (only green bars), Balanced LOLE: Power generation from FRE and flexibility options (all colored bars).

Both plots show significant, detailed impacts of flexibility options and curtailment which are the causes for the less values of the balanced LOLE compared to the constrained LOLE.

Chapter 5

Conclusion

This thesis presents an analysis for system reliability of a German energy scenario for 2025 in conjunction with various meteorological years and applying an energy system model.

In the first part of this thesis, the methodology for calculating the loss of load expectation (LOLE) as a metric of system reliability is described. The suitability of using system reliability for analyzing the impact of weather conditions is based on an extensive literature review documented in chapter 2.

For analyzing the impact of weather conditions, each meteorological year, characterized by its potential electricity generation time series of fluctuating renewable energy sources (GFRE), is analyzed by several statistical indicators. In order to assess the annual fluctuation of each year hourly gradients of each time series are calculated. Furthermore, hourly power generation can be used to derive the yearly amount of energy generated from fluctuating renewable sources. The analysis of the differences in the annual amounts of energy during the investigated time period (2006 - 2012), gives an evidence of the fluctuation during all seven meteorological years.

As stated in chapter 1, one main objective of this thesis is to assess the influence of weather conditions on system reliability. To determine this, a constrained single node German energy system without balancing options is considered. Seven scenarios, using various meteorological years as input, are applied to calculate the constrained LOLE for 2025. On average, a LOLE of 54 hours per year is determined. The average as well as each separate LOLE is over 2.4 hours per year. Based on

5. Conclusion

the requirements for system reliability stated in [7], the constrained German energy system therefore is not reliable.

Considering an energy scenario with high shares of fluctuating renewable energy (FRE) sources, the presumption arises, that the influence of weather data is significant and measurable. The outcome of this analysis confirms the formulated hypothesis. The results of the constrained single node German energy system without balancing show an annual variation of the LOLE of 15.5 % from the average LOLE during the considered time period and therefore imply a large influence of weather data on the LOLE. Besides determining the impact of various meteorological years, a correlation between the weather data and system reliability can be observed. Using a meteorological year with a high amount of annual power generation by FRE sources, a low LOLE results, which indicates a higher reliability of the energy system. Also a positive correlation between the fluctuation of power generation by FRE sources in a meteorological year and the LOLE can be observed. This means, if the yearly fluctuation of a weather year is high, a high value for the LOLE is determined.

For the balanced LOLE approach, the energy system model REMix is applied. Due hourly dispatch optimization and balancing options the average system reliability of a German energy system for 2025 gains 0.8 minutes (0.0135 hours) and thus the industry standard for a reliable system is met.

The analysis of the influence of meteorological years on the balanced LOLEs can not be captured as clear as the impact on the constrained LOLE. The fluctuation of the balanced LOLE during all seven years is about 109.5 % of the average value. As stated in 4.6.1, this high fluctuation is a result of balancing the load time series. However, the balanced LOLEs have a negative correlation with the annual amounts of energy generated by FRE sources as well. Compared to the constrained LOLE the correlation is weaker. In contrast, the correlation between the annual fluctuations and the balanced LOLE is only slightly lower. Hence the ability of the hourly dispatch optimization is better compensating fluctuating amounts of energy generated by FRE than annual hourly fluctuations.

Another objective of this thesis is to analyze the influence of load balancing on system reliability. Therefore, the constrained LOLE is compared with the balanced LOLE. The results, discussed in subsection 4.6.2, confirm a large influence of load balancing on system reliability. The analysis showed a reduction of the balanced

LOLE values compared to the LOLEs of a constrained energy system without flexibility options, by nearly 100 %. It has been found, that electricity export and import as well as storage have a high contribution to the system reliability of the investigated energy scenario. For this energy system it can be summarized that different meteorological years have a significant less impact on system reliability when flexibility options are taken into account.

Chapter 6

Outlook

Several aspects for further work and suggestions for improvements can be identified. These aspects can be assigned to three different categories, which are namely the analysis of meteorological years, the REMix scenario and the analysis of system reliability.

6.1. Analysis of meteorological years

In this thesis, seven successive years have been used for analyzing correlations between meteorological years and system reliability. To support the statements of this thesis, it is proposed to apply more meteorological years to achieve more comprehensive information about yearly fluctuating weather patterns and how they affect energy systems.

In addition, it is suggested to develop a synthetic and typical weather year. As mentioned in chapter 1, the energy system model REMix uses often only one meteorological year as data input. In this case it would be advantageous to use a representative weather year for all related studies, so that the analyzed focus is minimally affected by the selection of a certain meteorological year.

6.2. REMix scenario

In section 4.6.2, the impact of curtailment and load balancing caused by flexibility options is analyzed. The considered flexibility options include not all possible options for load balancing. For a more detailed analysis, it is suggested to capture more available flexibilities such as electricity exports, imports and electrical storage. In addition, controlled charging of electric mobility, demand response, power-controlled cogeneration as well as thermal storage should be taken into account.

Another suggestion for further improvement is to consider run of river hydro (RRH) as FRE source. As mentioned in section 3.6, RRH is not treated as fluctuating source like photovoltaic and wind power due to a lack of data. Even though RRH power is not as weather depending as photovoltaic and wind power, while using GFRE for analyzing the influence of several meteorological years it is advantageous to capture all weather depending energy sources including RRH. Therefore further research is suggested to obtain sufficient data, so it is possible to use RRH power as fluctuating and weather dependent energy source as well.

For this thesis Germany is considered as single node. For further improvements Germany should be analyzed not as a single node but at least divided into transmission system operator regions. By dividing Germany in twenty nodes, national spatial and temporal load shifting is captured.

6.3. Analysis of system reliability

By now, all calculations of system reliability indicator LOLE are based on the load time series of the year 2010. As mentioned in section 3.6, the primary focus of this thesis is on the influence of weather depending generation time series of FRE sources, thus the load time series remains the same for each LOLE calculation. By more focusing on analyzing system reliability to determine verified predications about security of energy supply it is suggested to vary the load time series or to base it at least on the same year as the used GFRE.

For further analysis of system reliability it is also advisable to investigate system reliability not only considering various meteorological years, but in addition investigating several power plant portfolios. It is suggested to analyze the impact of dif-

ferent penetration rates of FRE sources on system reliability as well as the impact of different dispatchable power plant portfolios.

Bibliography

- [1] BMWi. Erneuerbare Energien auf einen Blick, 2014.
<http://www.bmwi.de/DE/Themen/Energie/Erneuerbare-Energien/erneuerbare-energien-auf-einen-blick.html> Accessed: 06.09.2015.
- [2] F. Borggreffe, T. Pregger, H. C. Gils, K. K. Cao, M. Deissenroth, S. Bothor, M. Blesl, U. Fahl, M. Steurer, and M. Wiesmeth. Kurzstudie zur kapazitätsentwicklung in süddeutschland bis 2025 unter berücksichtigung der situation in deutschland und den europäischen nachbarstaaten. Technical report, Deutsches Zentrum für Luft- und Raumfahrt, Institut für Energiewirtschaft und rationelle Energieanwendung der Universität Stuttgart im Auftrag des Umweltministeriums Baden-Württemberg, 2014.
- [3] S. Boslaugh. *Statistics in a nutshell*. O'Reilly Media, Sebastopol, CA, 2012.
- [4] A. S. Brouwer, M. Van Den Broek, A. Seebregts, and A. Faaij. Impacts of large-scale intermittent renewable energy sources on electricity systems, and how these can be modeled. *Renewable and Sustainable Energy Reviews*, 33:443–466, 2014.
- [5] Bundesregierung. Energiewende, 2015.
<http://www.bundesregierung.de/Content/DE/StatischeSeiten/Breg/Energiekonzept/0-Buehne/ma%C3%9Fnahmen-im-ueberblick.html>
Accessed: 05.06.2015.
- [6] Consentec GmbH, r2b energy consulting GmbH. Versorgungssicherheit in Deutschland und seinen Nachbarländern: länderübergreifendes Monitoring und Bewertung. Technical report, Consentec GmbH, r2b energy consulting GmbH, 2015.
- [7] D. Corbus, J. King, T. Mousseau, R. Zavadil, B. Heath, L. Hecker, J. Lawhorn, D. Osborn, J. Smit, R. Hunt, et al. Eastern wind integration and transmission study. *NREL* (<http://www.nrel.gov/docs/fy09osti/46505.pdf>), CP-550-46505, 2010.
- [8] Daniel Stetter. *Enhancement of the REMix energy system model: Global renewable energy potentials, optimized power plant siting and scenario*

- validation*. PhD thesis, Universität Stuttgart, 2014. (unveröffentlicht, im Entwurf).
- [9] Diego Luca de Tena. *Large Scale Renewable Power Integration with Electric Vehicles*. PhD thesis, Universität Stuttgart, 2014.
- [10] EnerNex Corporation. Final Report - 2006 Minnesota Wind Integration Study. Technical report, EnerNex Corporation, 2006.
- [11] ENTSO-E. Hourly load values of all countries for a specific month. <https://www.entsoe.eu/db-query/consumption/mh1v-all-countries-for-a-specific-month> Accessed: 07.05.2015.
- [12] ENTSO-E. Specific national considerations, 2015. https://www.entsoe.eu/Documents/Publications/Statistics/Specific_national_considerations.pdf Accessed: 11.08.2015.
- [13] Eurostat. Electricity production, consumption and market overview, 2015. http://ec.europa.eu/eurostat/statistics-explained/index.php/Electricity_production,_consumption_and_market_overview Accessed: 02.06.2015.
- [14] GB Powertech. Verfügbarkeit von Wärmekraftwerken 2004 - 2013. Technical report, VGB Powertech e. V. Essen, 2014.
- [15] GE Energy. Western Wind and Solar Integration Study. Technical report, 2010.
- [16] Hans Christian Gils. *Balancing of Intermittent Renewable Power Generation by Demand Response and Thermal Energy Storage*. PhD thesis, Universität Stuttgart, 2015.
- [17] B. Hasche, A. Keane, and M. O'Malley. Capacity value of wind power, calculation, and data requirements: the Irish power system case. *Power Systems, IEEE Transactions on*, 26(1):420–430, 2011.
- [18] K. C. Hoffman and D. O. Wood. Energy system modeling and forecasting. *Annual review of energy*, 1(1):423–453, 1976.
- [19] A. Keane, M. Milligan, C. J. Dent, B. Hasche, C. D'Annunzio, K. Dragoon, H. Holttinen, N. Samaan, L. Söder, and M. O'Malley. Capacity value of wind power. *Power Systems, IEEE Transactions on*, 26(2):564–572, 2011.
- [20] A. Kumar, S. Sehgal, D. Arora, and A. Soni. Capacity outage probability table calculation (COPT) of Haryana Power Generation Corporation Limited using VBA. *International Journal of Technical Research (IJTR)*, 2:6–11, 2013.
- [21] P. McGraw Hill Financial. World Electric Power Plants Database, 2015.

-
- [22] J. Michaelis, P. Plötz, and S. Müller. The influence of individual wind feed-in time series on electricity spot market prices and their effect on the economic evaluation of storage systems. *Conference paper for the 14th IAAE European Energy Conference 2014*, 2014.
- [23] Pentalateral Energy Forum Support Group 2. Generation adequacy assessment. Technical report, Pentalateral Energy Forum Support Group 2, 2015.
- [24] H. Phoon. Generation system reliability evaluations with intermittent renewables. *a thesis of Master of Science in energy systems and the environment, University of Strathclyde*, 2006.
- [25] J. F. Prada. The value of reliability in power systems-pricing operating reserves. 1999.
- [26] Y. Scholz. *Renewable energy based electricity supply at low costs: development of the REMix model and application for Europe*. PhD thesis, Universität Stuttgart, 2012.
- [27] U.S. Energy Information Administration. World energy consumption, 2013. <http://www.eia.gov/todayinenergy/detail.cfm?id=12251> Accessed: 05.09.2015.
- [28] X. Wang and J. R. McDonald. *Modern power system planning*. McGraw-Hill Companies, 1994.

Appendices

Appendix A

Capacity outage probability table

COPT Python script

```
# Definitions: 'outCap' = X (outage Capacity), n = number of units, 'exactProb' = P
(X) (exact Probability that X is on outage), 'cumProb' = P(X>=) (Probability
that the outage is equal or more than X), 'Pn-1' = Pn-1(X>=) (Probability that
the outage of all already added units is equal or more than X), 'Pn-1(X-C)' =
Pn-1((X-C)>=) (Probability that the outage of all already added units is equal
or more than X-C (C = Capacity of the new unit))
# The COPT is calculated iterative. With each step row by row gets filled with
calculated values. This script calculates primarily the cumulative probability.
So 'Pn-1' is the probability that more than 'outCap' is on outage. The exact
probability is calculated from the cumulative probabilities.

# Import of used Python libraries
import pandas as pd
from pandas import ExcelWriter
import time
import numpy as np

start_time = time.time()      # Start clock

step = 1      # Step increment for margin states

data = pd.read_excel("PlantData_2025.xlsx", header=0, index_col=0) # Read in Excel
file as DataFrame

# Name columns of COPT
rowData = {'state': None,
          'availableCap': None,
          'outageCap': None,
          'Pn-1': None,
          'Pn-1(X-C)': None,
          'x-c': None,
          'exactProb': None,
          'cumProb': None,
          }

curTotCap = 0
```

A. Capacity outage probability table

```
sysCap = 0

sysCap = (data['Unit Size (MW)'] * data['No. Of Units']).sum() # Calculate energy
system's capacity

sysCap = sysCap + 2 # The value of sysCap is going to be the number of states (
rows of COPT). The first state has to be zero (0 outageCap) and the last state
need to be syscap + 1. This state is a auxiliary state, to calculate the exact
probability of the second last state.

outData = pd.DataFrame(np.zeros((sysCap, len(rowData.keys()))), columns=rowData.
keys()) # Create DataFrame with rowData as columns and fill DataFrame with
zeros for as much rows as the value of sysCap. The COPT filled with zeros is
the initialisation.

# Loop to get number of unit, unit size and FOR
for idx, irow in data.iterrows():
    units = irow['No. Of Units']
    newCap = irow['Unit Size (MW)']
    forc = irow.FOR

# Loop to add unit by unit to the COPT
for iunit in range(1, units+1):
    curTotCap += newCap # Current total capacity (CurtotCap) is increased
    by the unit size of the new Unit
    outageCap = 0 # Starting point: Outage capacity is zero
    pn = 1 # Initialisation of auxiliary variable

    while pn > 0:
        outData.loc[outageCap]['state'] = outageCap
        outData.loc[outageCap]['availableCap'] = curTotCap - outageCap
        outData.loc[outageCap]['outageCap'] = outageCap
        outData.loc[outageCap]['x-c'] = outageCap - newCap

        if outageCap == 0:
            outData.loc[outageCap]['Pn-1'] = 1 # Pn-1(X>=) = 1
        else:
            outData.loc[outageCap]['Pn-1'] = outData.loc[outageCap, 'cumProb'] #
            Pn-1(X>=) is the 'cumProb' (P(X>=)) of the previous unit state

        if outData.loc[outageCap]['x-c'] <= 0:
            outData.loc[outageCap]['Pn-1(X-C)'] = 1 # If X <= C "it is
            stipulated that 'Pn-1(X-C)' = 1"
        else:
            deltas = abs(outData['outageCap'] - outData.loc[outageCap]['x-c']) #
            Finding the index of data entry in column 'outcap' which is
            equal with 'x-c'. This index = curID
            location = deltas == 0
            curID = outData[location]['outCap']
            outData.loc[outageCap]['Pn-1(X-C)'] = outData.loc[curID]['Pn-1'] #
            Getting the Probability of Pn-1((X-C)>=) for the current 'state'.
            This probability is equal to Pn-1(X>=) where X-C of the current
            state is equal to X of a prvious state.
```

```

outData.loc[outageCap]['cumProb'] = outData.loc[outageCap]['Pn-1'] * (1
- forc) + outData.loc[outageCap]['Pn-1(X-C)'] * forc # Exprese
Equation 3.1 (subsection 3.1.1)

if outageCap > 0:
    outData.loc[outageCap-1]['exactProb'] = outData.loc[outageCap-1]['
cumProb'] - outData.loc[outageCap]['cumProb'] # Example: P(X=3)
= P(X>=3) - P(X>=4), P(X=3) = (1-P(X<3)) - (1-P(X<4)), P(X=3) =
P(X<4) - P(X<3)

pn = outData.loc[outageCap]['cumProb']

outageCap += step # Increase outage capacity by step increment

print("--- %s seconds ---" % (time.time() - start_time)) # End clock, print time

# Write COPT DataFrame to Excel file
writer = ExcelWriter("COPT_2025.xlsx")
outData.to_excel(writer, "COPT", index=False)
writer.save()

```

A. Capacity outage probability table

Sections of the COPT

Table A.1.: Sections of the computed capacity outage probability table.

Out Cap (MW)	Available Cap (MW)	Pn-1	Pn-1(X-C)	x-c (MW)	Exact Prob	Cum Prob
0	62,907	1	1	-158	2.57×10^{-12}	1
1	62,906	1	1	-157	0	1
2	62,905	1	1	-156	0	1
3	62,904	1	1	-155	0	1
4	62,903	1	1	-154	0	1
5	62,902	1	1	-153	0	1
6	62,901	1	1	-152	0	1
7	62,900	1	1	-151	0	1
8	62,899	1	1	-150	0	1
9	62,898	1	1	-149	0	1
10	62,897	1	1	-148	0	1
11	62,896	1	1	-147	7.08×10^{-12}	1
12	62,895	1	1	-146	0	1
13	62,894	1	1	-145	0	1
14	62,893	1	1	-144	0	1
15	62,892	1	1	-143	0	1
16	62,891	1	1	-142	1.96×10^{-11}	1
17	62,890	1	1	-141	0	1
18	62,889	1	1	-140	0	1
19	62,888	1	1	-139	0	1
20	62,887	1	1	-138	0	1
21	62,886	1	1	-137	0	1
22	62,885	1	1	-136	9.67×10^{-12}	1
23	62,884	1	1	-135	0	1
...
3,964	58,943	0.626401	0.672976	3,806	0.000298	0.629429
3,965	58,942	0.626102	0.672687	3,807	0.000297	0.629130
3,966	58,941	0.625805	0.672398	3,808	0.000295	0.628833
3,967	58,940	0.625509	0.672108	3,809	0.000300	0.628538
3,968	58,939	0.625209	0.671816	3,810	0.000301	0.628238
3,969	58,938	0.624907	0.671523	3,811	0.000295	0.627937
3,970	58,937	0.624611	0.671235	3,812	0.000298	0.627642
3,971	58,936	0.624313	0.670946	3,813	0.000301	0.627344
3,972	58,935	0.624012	0.670651	3,814	0.000297	0.627043
3,973	58,934	0.623714	0.670361	3,815	0.000298	0.626746
...
55,164	7,743	1.63×10^{-208}	1.10×10^{-205}	55,006	3.19×10^{-208}	7.33×10^{-207}
55,165	7,742	1.58×10^{-208}	1.06×10^{-205}	55,007	2.73×10^{-208}	7.01×10^{-207}
55,166	7,741	1.50×10^{-208}	1.01×10^{-205}	55,008	2.59×10^{-208}	6.73×10^{-207}
55,167	7,740	1.44×10^{-208}	9.76×10^{-206}	55,009	2.95×10^{-208}	6.48×10^{-207}
55,168	7,739	1.39×10^{-208}	9.31×10^{-206}	55,010	2.15×10^{-208}	6.18×10^{-207}
55,169	7,738	1.32×10^{-208}	8.99×10^{-206}	55,011	2.46×10^{-208}	5.97×10^{-207}
55,170	7,737	1.28×10^{-208}	8.62×10^{-206}	55,012	2.45×10^{-208}	5.72×10^{-207}
55,171	7,736	1.22×10^{-208}	8.25×10^{-206}	55,013	1.89×10^{-208}	5.48×10^{-207}
55,172	7,735	1.17×10^{-208}	7.97×10^{-206}	55,014	2.47×10^{-208}	5.29×10^{-207}
55,173	7,734	1.13×10^{-208}	7.59×10^{-206}	55,015	1.87×10^{-208}	5.04×10^{-207}
...
62,901	6	0	0	62,743	0	0
62,902	5	0	0	62,744	0	0
62,903	4	0	0	62,745	0	0
62,904	3	0	0	62,746	0	0
62,905	2	0	0	62,747	0	0
62,906	1	0	0	62,748	0	0
62,907	0	0	0	62,749	0	0
62,908	-1	0	0	62,750	0	0

Appendix B

Loss of load expectation Python script

```
# Import of used Python libraries
import pandas as pd
from pandas import ExcelWriter
import glob
import re
import numpy as np
from matplotlib import pyplot as plt

fileList = glob.glob('*.xlsx') # List all .xlsx files (Residual load time series)
                                in directory

# Define natural_sort
def natural_sort(l):
    convert = lambda text: int(text) if text.isdigit() else text.lower()
    alphanum_key = lambda key: [convert(c) for c in re.split('([0-9]+)', key)]
    return sorted(l, key = alphanum_key)

sortFileList = natural_sort(fileList) # Sort list

dataC = pd.read_excel("COPT/COPT_2025.xlsx", header=0, index_col=None) # Read in
Excel file as DataFrame
dataC = dataC.set_index('state') # Set 'state' as index
allLOLE = pd.DataFrame() # Create empty DataFrame for all LOLEs

# Loop to get each file in list
for iName in sortFileList:
    dataL = pd.read_excel(iName, header=0) # Read in excel file as DataFrame
    year = iName[19:-5] # Capture year
    print(year)

    dataL = np.round(dataL, decimals=0) # Round up to 0 decimal digits

# Name columns of LOLP table
rowData = {'outageCap': None,
           'prob': None,
           'time': None,
           'LOLP': None,
           }
```

B. Loss of load expectation Python script

```
LOLPTable = pd.DataFrame(columns=rowData.keys()) # Create DataFrame with
rowData as columns

maxInst = float(dataC.iloc[0]['availableCap']) # Set maxInst to '
availableCap' of state 0
maxLoad = float(dataL[['Residual Load']].max(0)) # Set maxLoad to maximum of '
Residual Load'
reserve = float(maxInst - maxLoad) # Calculate reserve

sortDataRL = dataL.sort(['Residual Load'], ascending=False) # Sort 'Residual
Load' descending
idx = [i for i in range(0, (len(dataL)))] # Create list counting from 0 to
length of dataL (8759)
sortDataRL[''] = idx # Set idx as column ''
sortDataRL = sortDataRL.set_index('') # Set column '' as index

idx = [i for i in range(1, (len(dataL)+1))] # Create list counting from 1 to
8760
sortDataRL['Hour'] = idx # Set list as column 'Hour'

LOLPsum = 0

# Loop to go through COPT row by row
for idx, irow in dataC.iterrows():
    outCap = irow['outageCap']
    Prob = irow['exactProb']

    if outCap > reserve:
        rowData['outageCap'] = outCap
        rowData['prob'] = Prob

    if sortDataRL.loc[sortDataRL['Residual Load'] == (maxInst - outCap)].
        empty == True: # If no value in 'Residual Load' is equal to (maxInst
        - outCap)
        rowData['outageCap'] = 0
        rowData['prob'] = 0
        rowData['time'] = 0
        rowData['LOLP'] = 0
    else:
        idC = sortDataRL.loc[sortDataRL['Residual Load'] == (maxInst -
        outCap)].index # Value in 'Residual Load' is equal to (maxInst -
        outCap), index of this value is stored in idC
        m = sortDataRL.loc[idC, 'Hour'] # m = Value in colum 'Hour'
        of index idC
        maIn = max(m)
        time = float(maIn) / (len(dataL)) # time in which the outage of
        outCap causes a loss of load (Hour / 8760 h)
        rowData['time'] = time # LOLP table is filled
        rowData['LOLP'] = time * Prob
        LOLPsum += rowData['LOLP'] # Summing up LOLPsum
```

```

else:                                     # If outCap is smaller than
    reserve
    rowData['outageCap'] = 0
    rowData['prob'] = 0
    rowData['time'] = 0
    rowData['LOLP'] = 0

    LOLPTable = LOLPTable.append(rowData, ignore_index=True) # Append new row
    to DataFrame LOLPTable

LOLPTabSlim = LOLPTable.loc[~LOLPTable.apply(lambda row: (row==0).all(), axis
=1)] # Removes all rows which are 0

outPut = pd.DataFrame({'LOLE in hours/year': [LOLPsum * (len(dataL))])} #
    Calculate LOLE
outPut['LOLE in hours/year'] = np.round(outPut['LOLE in hours/year'], decimals
=2) # Round up to 2 decimal digits

allLOLE[year] = outPut['LOLE in hours/year'] # Write LOLE in DataFrame with
    all LOLEs

print('Building: Constrained Results/ConstLOLPTable_2025_' + year + '.xlsx')

# Write LOLP table DataFrame to Excel file
writer = ExcelWriter('Results/ConstLOLPTable_2025_' + year + '.xlsx') #
    Speichert df als .xlsx (=LOLP Tabelle und LOLE Value)
LOLPTabSlim.to_excel(writer, 'LOLP Table', index=False)
outPut.to_excel(writer, 'LOLE', index=False)
writer.save()

# Rename and transform all LOLEs DataFrame
allLOLE['Year'] = ['LOLE in hours/year']
allLOLE = allLOLE.set_index('Year')
allLOLE = allLOLE.T

# Write all LOLEs DataFrame to Excel file
writer = ExcelWriter('Results/LOLE_all_years.xlsx')
allLOLE.to_excel(writer, 'LOLE', index=True)
writer.save()

```


Appendix C

REMix input

Table C.1.: Installed capacities of dispatchable power plants in Europe 2025.

Country	Technology	Installed Capacity (MW)
Austria	Biomass	1,118
	CCGT	1,618
	GT-NGas	1,359
	ST-Coal	461
	ST-Lignite	0
	ST-Nuclear	0
Belgium	Biomass	1,775
	CCGT	7,974
	GT-NGas	1,073
	ST-Coal	1,158
	ST-Lignite	0
	ST-Nuclear	2,825
CzechRep	Biomass	666
	CCGT	1,660
	GT-NGas	470
	ST-Coal	2,458
	ST-Lignite	5,497
	ST-Nuclear	3,731
Denmark East	Biomass	858
	CCGT	0
	GT-NGas	0
	ST-Coal	0
	ST-Lignite	0
	ST-Nuclear	0
Denmark West	Biomass	286
	CCGT	979
	GT-NGas	1,112
	ST-Coal	1,447
	ST-Lignite	0
	ST-Nuclear	0
France	Biomass	4,260
	CCGT	6,943
	GT-NGas	4,880
	ST-Coal	369
	ST-Lignite	0
	ST-Nuclear	40,455
Germany	Biomass	896
	CCGT	17,903
	GT-NGas	2,191
	ST-Coal	18,738
	ST-Lignite	1,3619

C. REMix input

Italy	ST-Nuclear	0
	Biomass	3,614
	CCGT	41,588
	GT-NGas	9,308
	ST-Coal	2,755
Luxemburg	ST-Lignite	0
	ST-Nuclear	0
	Biomass	91
	CCGT	398
	GT-NGas	26
Netherlands	ST-Coal	0
	ST-Lignite	0
	ST-Nuclear	0
	Biomass	2,111
	CCGT	1,6941
Norway	GT-NGas	1,809
	ST-Coal	4,875
	ST-Lignite	0
	ST-Nuclear	434
	Biomass	971
Poland	CCGT	1,858
	GT-NGas	1,486
	ST-Coal	621
	ST-Lignite	0
	ST-Nuclear	2,385
Sweden	CCGT	873
	GT-NGas	133
	ST-Coal	8,606
	Biomass	1,294
	ST-Lignite	6,339
Switzerland	ST-Nuclear	0
	Biomass	4,447
	CCGT	0
	GT-NGas	0
	ST-Coal	0
	ST-Lignite	0
	ST-Nuclear	0
	Biomass	1,000
	CCGT	151
	GT-NGas	392
	ST-Coal	0
	ST-Lignite	0
	ST-Nuclear	2,055

Table C.2.: Installed capacities of pumped storage power plants in Europe 2025.

Country	Technology	Installed Converter (MW)	Installed Storage (MWh)
Austria	Pumped Storage	4,285	29,995
Belgium	Pumped Storage	1,310	9,170
Czech Republic	Pumped Storage	1,150	8,047
Denmark East	Pumped Storage	0	0
Denmark West	Pumped Storage	0	0
France	Pumped Storage	3,954	27,678
Germany	Pumped Storage	9,560	66,920
Italy	Pumped Storage	6,437	45,060
Luxemburg	Pumped Storage	1,295	9,065
Netherlands	Pumped Storage	0	0
Norway	Pumped Storage	1,027	7,186
Poland	Pumped Storage	1,466	10,263
Sweden	Pumped Storage	430	3,010
Switzerland	Pumped Storage	3,793	26,551

Table C.3.: Installed capacities of fluctuating renewable energy sources in Europe 2025.

Country	Technology	Installed Capacity (MW)
Austria	Run of River Hydro	6,888
	Photovoltaic	874
	Wind Offshore	0
	Wind Onshore	4,507
Belgium	Run of River Hydro	178
	Photovoltaic	4,295
	Wind Offshore	2,346
	Wind Onshore	3,518
CzechRep	Run of River Hydro	454
	Photovoltaic	2,042
	Wind Offshore	0
	Wind Onshore	352
Denmark East	Run of River Hydro	0
	Photovoltaic	511
	Wind Offshore	1,050
	Wind Onshore	1,092
Denmark West	Run of River Hydro	12
	Photovoltaic	68
	Wind Offshore	1,556
	Wind Onshore	3,160
France	Run of River Hydro	16,935
	Photovoltaic	9,931
	Wind Offshore	9,841
	Wind Onshore	29,522
Germany	Run of River Hydro	4,161
	Photovoltaic	54,700
	Wind Offshore	8,900
	Wind Onshore	53,800
Italy	Run of River Hydro	15,256
	Photovoltaic	25,343
	Wind Offshore	1,981
	Wind Onshore	1,6024
Luxemburg	Run of River Hydro	43
	Photovoltaic	350
	Wind Offshore	0
	Wind Onshore	256
Netherlands	Run of River Hydro	68
	Photovoltaic	1,025
	Wind Offshore	7,076

C. REMix input

Norway	Wind Onshore	4,717
	Run of River Hydro	4,446
	Photovoltaic	376
	Wind Offshore	1,500
Poland	Wind Onshore	3,775
	Run of River Hydro	1,035
	Photovoltaic	350
	Wind Offshore	2,083
Sweden	Wind Onshore	6,248
	Run of River Hydro	6,153
	Photovoltaic	247
	Wind Offshore	197
Switzerland	Wind Onshore	4,740
	Run of River Hydro	4,394
	Photovoltaic	1,661
	Wind Offshore	0
	Wind Onshore	936

List of Figures

3.1.	Load duration curve 2010.	12
3.2.	Loss of load probability calculation.	13
3.3.	Basic structure of the REMix model.	16
3.4.	Comparison of input data for each loss of load expectation approach.	17
3.5.	Countries considered in the REMix scenarios applied for the balanced loss of load expectation approach.	21
3.6.	Installed capacities in Germany in 2025.	22
4.1.	Box plot of several indicators for characterizing the potential electricity generation time series of fluctuating renewable energy sources for each meteorological year.	27
4.2.	Potential amount of energy generated by fluctuating renewable energy sources in Germany of each meteorological year.	28
4.3.	Box plot of several indicators for characterizing the hourly gradients of the potential electricity generation time series of fluctuating renewable energy sources for each meteorological year.	30
4.4.	Frequency distribution of absolute hourly gradients of the potential electricity generation time series of photovoltaic power 2011.	33
4.5.	Frequency distribution of absolute hourly gradients of the potential electricity generation time series of wind offshore power 2011.	33
4.6.	Frequency distribution of absolute hourly gradients of the potential electricity generation time series of wind onshore power 2011.	34
4.7.	Frequency distribution of absolute hourly gradients of the potential electricity generation time series of fluctuating renewable energy sources 2011.	35
4.8.	Residual load duration curves, load curve and installed capacity used for calculating the constrained loss of load expectation.	36
4.9.	Balanced residual load duration curves, load curve and installed capacity used for calculating the balanced loss of load expectation.	38
4.10.	Balanced residual load duration curves of the first 40 hours.	39
4.11.	Residual load duration curves, load curve and installed capacity used for calculating the both loss of load expectations.	45

4.12. Hourly dispatch of certain technologies for Germany on 24 and 25 May 2025 – Constrained LOLE: Power generation from FRE (only green bars), Balanced LOLE: Power generation from FRE and flexibility options (all colored bars).	46
4.13. .: Hourly dispatch of certain technologies for Germany on 20 and 21 December 2025 – Constrained LOLE: Power generation from FRE (only green bars), Balanced LOLE: Power generation from FRE and flexibility options (all colored bars).	47

List of Tables

3.1.	Example capacity outage probability table calculation.	10
3.2.	Data sources.	19
3.3.	Dispatchable power plant data of Germany.	20
4.1.	Characterization of the hourly potential electricity generation time series of fluctuating renewable energy sources for each meteorological year.	26
4.2.	Amount of potential energy generated by fluctuating renewable energy sources of each meteorological year.	27
4.3.	Characterization of absolute hourly gradients of the potential electricity generation time series of fluctuating renewable energy sources for each meteorological year.	29
4.4.	Potential number of full load hours of each technology of each meteorological year.	31
4.5.	Normalized hourly mean gradients of the potential electricity generation time series of each technology of each meteorological year.	32
4.6.	Constrained loss of load expectation for 2025 of each meteorological year.	35
4.7.	Balanced loss of load expectation for 2025 of each meteorological year.	37
4.8.	Correlation between the potential electricity generation time series of fluctuating renewable energy sources and the constrained loss of load expectation for 2025.	40
4.9.	Correlation between the potential electricity generation time series of fluctuating renewable energy sources and the balanced loss of load expectation for 2025.	41
4.10.	Constrained and balanced loss of load expectation for 2025 of each meteorological year.	44
A.1.	Sections of the computed capacity outage probability table.	66
C.1.	Installed capacities of dispatchable power plants in Europe 2025.	71
C.2.	Installed capacities of pumped storage power plants in Europe 2025.	73
C.3.	Installed capacities of fluctuating renewable energy sources in Europe 2025.	73

